The ILC Physics Case

W. Kilian[1] and P. M. Zerwas[2]

1- Fachbereich Physik, Universität Siegen, D-57068 Siegen, Germany

2- Deutsches Elektronen-Synchrotron DESY, D-22603 Hamburg, Germany
Inst. Theor. Physik E, RWTH Aachen, D-52074 Aachen, Germany
Laboratoire de Physique Théorique, U. Paris-Sud, F-91405 Orsay, France

Experiments in the energy range from the scale of electroweak symmetry breaking to the TeV scale are expected to be crucial for unraveling the microscopic structure of matter and forces. The high precision which should be achieved in experiments at lepton colliders, is a necessary ingredient for providing a comprehensive picture of the mechanism breaking the electroweak symmetries and generating mass, the unification of forces, involving most likely supersymmetry, and the structure of space-time at small distances. In addition, clarifying the nature of the particles which build up cold dark matter in the universe, needs a lepton collider to match the high experimental precision which will be reached in cosmology experiments.

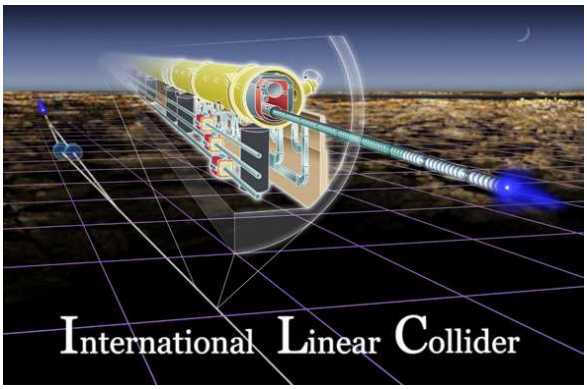

1 Introduction

High-energy physics has been tremendously successful in unraveling the basic laws of nature in the microcoscopic world. With the Standard Model of particle physics a picture has emerged which adequately describes the structure of matter and forces. However, this picture is still incomplete internally, and externally, driven by theoretical arguments and experimental observations, the model should be embedded in a more comprehensive theory which unifies the different degrees of freedom. These points lead us in a natural way to a set of crucial experimental questions. Answering these questions will unify our view of the microscopic world and thus deepen our understanding of the universe enormously.

Derived from our present knowledge of particle physics, solutions to the following problems, which are central to physics in general, must be approached experimentally:

- the mechanism responsible for breaking the electroweak symmetries and generating mass;
- the unification of forces, including gravity in the end;
- the structure of space-time at small distances.

This set of fundamental problems is complemented by a new branch in the development of particle physics:

- the connection to cosmology.

Besides the nature of particles which may form components of cold dark matter in the universe, several other problems connect microscopic physics and cosmology, the baryon asymmetry in the universe being a prominent example.

Based on the present picture of physics, the scientific value of any new accelerator is determined by the unique contributions the facility can offer in approaching solutions to these problems.

We are in the fortunate position that the next generation of accelerators holds the promise of providing answers to these questions indeed. They will greatly advance the understanding of the microscopic world in particular and the universe as a whole. With the Large Hadron Collider LHC, soon starting at CERN, a first decisive step will be taken. From this machine which will operate at the TeV energy frontier, we expect breakthrough discoveries in the complex of electroweak symmetry breaking and in the physics area beyond the Standard Model. However, this hadron facility must be complemented with a lepton collider which will play a key role in drawing a comprehensive and high-resolution picture of electroweak symmetry breaking and of the physics layer underneath the Standard Model. Our present knowledge of physics is expected to converge to a unified picture in this layer.

The e^+e^- Linear Collider ILC, which is now in the design phase, would be the counterpart in a tandem with LHC, cf. Refs. [2, 3]. In analogy to the relation between LEP and Tevatron, the ILC energy of 1 TeV in the lepton sector is equivalent in many aspects to the higher LHC energy, effectively about 5 TeV in the quark sector. Moreover, by including the characteristic scale of electroweak symmetry breaking, the ILC covers one of the most crucial energy domains in particle physics. Discoveries at LHC may also point to physics scales beyond the reach of ILC; this area could be accessed by a multi-TeV e^+e^- facility [4].

1.1 Physics scenarios

Electroweak symmetry breaking and Higgs mechanism

The mechanism which breaks the electroweak symmetries, is the still missing cornerstone of the Standard Model. High-precision analyses strongly suggest the Higgs mechanism, including a light Higgs boson, to be responsible for the breaking of the electroweak symmetries and for generating the masses of the fundamental particles [5]. If the Higgs boson will be discovered at LHC, it must be established experimentally that this mechanism is indeed responsible for generating the masses of the particles. The precision with which this question can be answered at ILC, exceeds the LHC by an order of magnitude. In addition, in the most probable light mass range ILC provides the unique opportunity for establishing the Higgs self-energy potential, which is the essential *agens* for inducing the symmetry breaking.

In extensions of the Standard Model, like supersymmetric theories or Little Higgs theories, the Higgs sector is much more complex. A spectrum of Higgs particles will in general be realized, demanding precision studies of masses, mixing and couplings to explore the structure of the Higgs sector.

If the standard Higgs mechanism, including a set of Higgs particles, were not realized in nature, but alternatively a higgs-less theory as suggested, for example, in theories of electroweak symmetry breaking by new strong interactions at low scales, cf. Ref. [6], such a scenario could be explored in the scattering of electroweak bosons at LHC and ILC. However, taking advantage of the less complex final-state topology at the lepton collider ILC, experiments at this machine can cover the entire threshold region of the new strong interactions and open the door to an arena of novel interactions. Other higgs-less scenarios, as formulated in some theories of extra space dimensions, also give rise to new interactions between the standard electroweak gauge bosons mediated by novel TeV scale resonances.

Unification and supersymmetry

Progress in particle physics has opened the path to the truly unified understanding of nature. The unification of the electromagnetic, weak and strong interactions is strongly indicated by the evolution of the couplings merging at high energies, cf. Refs. [7] , and expected to be joined by gravity in the ultimate unification near the Planck scale. A key role in the evolution is played by supersymmetry, cf. Ref. [8]. LHC has the potential to discover supersymmetry in the next few years, and the theoretical concept can be verified in conjunction with ILC which is an essential instrument in this process.

Supersymmetry embraces several of the fundamental points introduced at the beginning – providing a stable bridge between the scale of electroweak symmetry breaking and the Planck scale; leading to the unification of the standard couplings and paving the path for including gravity in particle physics. In addition, the lightest supersymmetric particle is a compelling candidate for forming a component of the large amount of cold dark matter observed in the universe. Thus, this theory could not only play a fundamental role in particle physics but also links particle physics closely with cosmology.

In fact, high-precision measurements of electroweak observables, combined with constraints from the observation of the cold dark matter density by WMAP, allow for a large area of fairly low-scale supersymmetry parameters, though no firm conclusions can be drawn as yet. In the favorable case a significant fraction of the non-colored supersymmetric particles, i.e., partners of the photon, of the electron etc, should be observed at ILC operating in the first phase at 500 GeV, and more in the upgraded 1 TeV phase of the machine. LHC would play the complementary role for colored particles, the supersymmetric partners of the quarks and gluons.

Quite generally, apart from exceptional corners of parameter space, LHC experiments will discover supersymmetric particles if this symmetry is realized in nature not far above the electroweak scale. However, the spectrum of particles in this new world that can be detected at LHC will remain incomplete, particularly in the light non-colored sector. Moreover, the precision in the determination of their properties, like masses, mixings and couplings, remains limited. Operating ILC will, first, lead to a comprehensive view of the spectrum of light particles and, second, improve the accuracy in measuring their properties by one to two orders of magnitude.

Both points are very important for several reasons. Foremost, the completeness of the

spectrum and the greatly improved accuracies will allow us to extrapolate the parameters to the unification scale where the fundamental supersymmetric theory and the microscopic picture of its breaking mechanism can be reconstructed.

This way we can study the structure of physics at scales close to the Planck scale. This provides us with the unique opportunity to shed light on an energy domain where the roots of particle physics in particular, and physics quite generally, may be located. Information on this area from other branches of particle physics, potentially proton decay experiments etc, will remain very scarce so that the telescope character of high-precision high-energy experiments, in coherent LHC+ILC analyses, is of very high value.

High precision is also required in exploring the properties of the lightest supersymmetric particle which may contribute to the observed density of cold dark matter in the universe. Anticipating improved results from cold dark matter measurements in the near future, the accuracy of a lepton collider will be needed for masses, mixings and couplings to match eventually the accuracy of cosmology data. In addition, once the particle properties are determined accurately, observed fluxes in astroparticle search experiments can be exploited to map the distribution of cold dark matter in the universe. Thus ILC experimental results could reach far beyond the domain of particle physics.

Extra space dimensions

If extra space dimensions in the universe, cf. Refs. [9, 10, 11], are realized already at low energies, the experimental determination of the fundamental scale of gravity and the number of dimensions are of central interest. Starting these analyses with LHC, the picture can be refined considerably at ILC. By varying the energy of the collider, these two characteristics of gravity and space-time at short distances can be disentangled. By observing masses and widths of excited graviton states in other scenarios, the length scale and the curvature in an additional fifth dimension of space-time can be determined.

Many other measurements could be performed in this area, e.g., measurements of the spin of gravity fields, mixings of scalar fields etc, so that a large set of observables could be exploited at ILC which, joined with LHC results, would enable us to zoom in on the underlying theoretical picture.

1.2 Basic experimental parameters

It is generally assumed that the International Linear Collider ILC will be operated in two phases. In the first phase the cm energy will reach $\sqrt{s} = 500$ GeV, in the second phase 1 TeV. In each of the phases a total integrated luminosity of about 1 ab^{-1} is expected to be accumulated when the runs are completed. The first phase gives access to light Higgs bosons, the top quark, light supersymmetric particles, the second phase to strong electroweak symmetry breaking, heavy new particles in the Higgs and supersymmetric sectors, extra space dimensions and other high-scale phenomena. Some scenarios may suggest extensions of the linear collider program beyond the TeV energy.

Experiments at ILC will focus on high-precision analyses. If the electron and positron beams are polarized, typically $P_{e^-} \sim 90\%$ and $P_{e^+} \sim 60\%$, the experimental potential of the machine can truly be exhausted, cf. Ref. [12]. In addition to longitudinally polarized beams, spin rotators can generate transversely polarized electron/positron beams. The polarization of the electron beam is a necessary condition for many experimental analyses while the

polarization of the positron beam is generally viewed as an auxiliary tool which however may turn out to be crucial in some special physics scenarios.

The luminosity in running the machine as an e^-e^- collider is significantly smaller as the electrons repel each other when the bunches of the two colliding beams traverse each other.

In addition to the high-energy electron-positron collider mode, the machine can be operated in the GigaZ mode. Running at low energies on top of the Z-boson resonance, some 1 billion events, i.e., a factor fifty more than at LEP, may be collected within a few months. Combined with W and *top* threshold analyses, this leads to the ultimate precision in the electroweak sector in the foreseeable future. Both electron and positron polarization is essential for these analyses.

Finally, by means of Compton back-scattering of laser light, the ILC can also be operated as an $e\gamma$ and $\gamma\gamma$ collider. A fraction of 80% of the incoming electron/positron energy can be transferred to the photon(s), cf. Ref. [13]. The spectrum is maximal at the upper edge if the incoming e^-/e^+ beam and the laser photon beam are longitudinally polarized with opposite helicities. In this way colliding $e\gamma$ and $\gamma\gamma$ experiments can be performed with 90% and 80% of the total e^+e^- energy, respectively, and about one third of the luminosity accumulating in a 20% margin below the maximum possible energy. In some scenarios these modes open up unique discovery channels for particles, in the Higgs and slepton sectors of supersymmetric theories, or in the particle towers of compositeness models, for example, cf. Ref. [14].

2 Electroweak symmetry breaking

Unraveling the mechanism which breaks the electroweak symmetries and generates the masses of the fundamental standard particles — electroweak gauge bosons, leptons and quarks — is one of the key problems of particle physics, cf. Refs. [15]. Theoretical realizations span a wide range of scenarios extending from weak to strong breaking mechanisms. Examples on one side are the Standard Model and its supersymmetric extension involving light fundamental Higgs fields, and new strong interaction models without a fundamental Higgs field on the other side. Symmetry breaking by specific boundary conditions for gauge fields in the compactification of extra space dimensions gives rise to higgs-less models. The forthcoming experiments at LHC will lead to a breakthrough in revealing the breaking mechanism and in making the first steps into this new territory while ILC should provide the comprehensive understanding of the theory underlying the breaking of the electroweak symmetries and the generation of mass. Thus the experimental solution of this problem at LHC and ILC will unravel one of the fundamental laws of nature.

2.1 Higgs mechanism in the Standard Model

The analysis of the precision electroweak data from LEP, SLC and elsewhere points clearly to a light mass value of the Higgs particle [17], if the electroweak symmetries are broken by the Higgs mechanism in the framework of the Standard Model:

$$M_H = 76^{+33}_{-24}\ \text{GeV} \ \text{ and } \ M_H < 144\,\text{GeV} \ \ (95\%\,\text{CL}). \tag{1}$$

The direct search for the SM Higgs boson at LEP has set a lower limit of 114 GeV on the Higgs mass [18].

The Higgs particle of the Standard Model is guaranteed to be discovered at LHC, cf. Ref. [19]. The combination of several channels in different mass ranges gives rise to a large significance for the detection, i.e., $> 5\sigma$ for an integrated luminosity of 30 fb^{-1}.

After the discovery of the Higgs particle, it must be established experimentally that the Higgs mechanism is responsible indeed for breaking the electroweak symmetries and for generating the masses of the fundamental particles. This requires the precise determination of the profile of the Higgs particle. First steps in model-independent analyses of its properties can be taken at LHC by performing precision measurements of the Higgs mass, the ratios of some of the Higgs couplings, and bounds on couplings [20].

At ILC a clean sample of Higgs events can be generated in Higgs-strahlung, $e^+e^- \to ZH$, and WW fusion, $e^+e^- \to \bar{\nu}\nu H$. The clear signals above small backgrounds, cf. Fig. 1, allow the model-independent high-precision determination of the Higgs profile, besides the

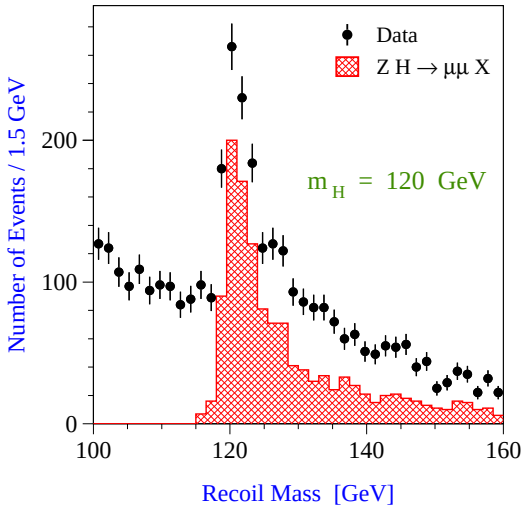

Figure 1: Signal and background of inclusive Higgs boson production in Higgs-strahlung; Ref. [21].

mass, the spin of the particle and, most important, its couplings, including the trilinear self-coupling in double-Higgs production. This information will be extracted from a set of production cross sections and angular distributions, and from decay branching ratios. Below a Higgs mass of 140 GeV a rich ensemble of final states can be studied; the ensemble of channels is reduced for heavier Higgs masses.

Higgs couplings

If the masses of the fundamental particles p are generated by the interaction with the Higgs field in the vacuum, the Higgs couplings must grow with the particle masses m_p:

$$g(Hpp) = (\sqrt{2}G_F)^{1/2} m_p. \qquad (2)$$

From the production cross sections for Higgs-strahlung and WW fusion the absolute values of the Higgs couplings to the electroweak gauge bosons Z and W can be determined in a model-independent way. Measuring the ratios of branching ratios involving quarks and leptons on one side, and the electroweak gauge bosons on the other side, also Higgs couplings to quarks and leptons can be determined in a model-independent way. A special case is the Higgs-top coupling which can be measured in Higgs radiation off top-quark pairs produced in e^+e^- annihilation. The accuracy which can be achieved for various couplings is predicted at the per-cent level [22]. How well the Higgs coupling – mass relation can be tested, is apparent from Fig. 2 which clearly demonstrates the linear relation between the Higgs couplings and

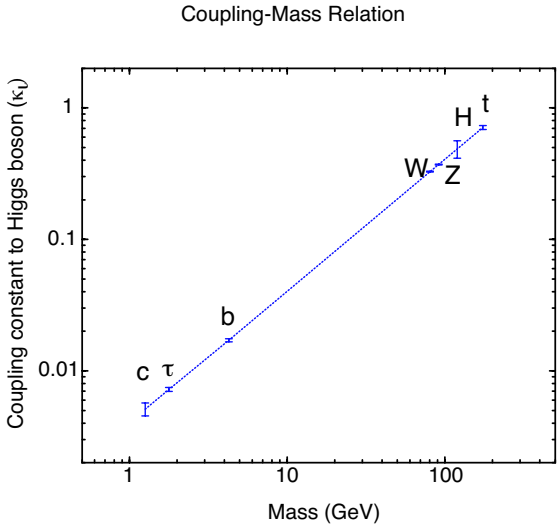

Figure 2: The relation between the Higgs coupling of a particle and its mass in the Standard Model; Ref. [23]. The error bars correspond to the accuracy expected from ILC data.

the masses for typical particle species in the Standard Model – electroweak gauge bosons, quarks and leptons, up and down types.

Higgs potential

The specific form of the Higgs potential, $V \sim [|\phi|^2 - v^2/2]^2$ shifts the ground state of the Higgs system to a non-zero field strength, $v/\sqrt{2}$. Specifying the direction of the field strength in charge space breaks the electroweak symmetries. The gauge and Yukawa interaction energy of other fields with the non-zero Higgs field in the vacuum can be reinterpreted as the mass of these particles. Expanding the potential about the minimum,

$$V = \frac{1}{2} M_H^2 H^2 + \frac{1}{2} \frac{M_H^2}{v} H^3 + \frac{1}{8} \frac{M_H^2}{v^2} H^4 \qquad (3)$$

the trilinear coupling plays the crucial role for the non-trivial shape of the potential. This parameter can be measured in the process of double-Higgs production, $e^+e^- \to ZHH$ and $\bar{\nu}\nu HH$,

as exemplified in Fig. 3. The product of small couplings and the large fraction of phase space absorbed by the masses render the production cross sections small. Nevertheless, the trilinear coupling is expected to be measured at ILC at a level of 12% for Higgs masses below about 140 GeV. The less crucial quartic coupling in the Standard Model seems out of reach for any collider in the foreseeable future. Thus the element in the Higgs potential which is most crucial for generating the Higgs medium in the ground state, can be reconstructed at ILC. In the upper intermediate Higgs mass range access to the trilinear coupling could be given by SLHC [25].

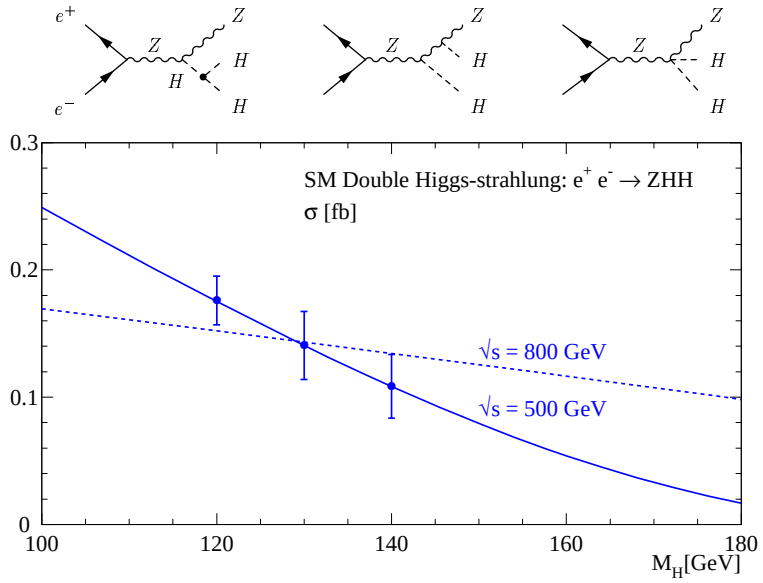

Figure 3: Cross section of Higgs pair production for measurements of the triple Higgs coupling; Ref. [24]. The error bars correspond to the accuracy expected from ILC data.

Direct measurements of the ZZH coupling to an accuracy of 1%, and of the HHH coupling to about 10%, give lower limits of about 3 and 1 TeV, respectively, for scales of new physics [26] . Since the microscopic dynamics of electroweak symmetry breaking is one of the central problems in particle physics, establishing these values would be a valuable and unique result of experiments at ILC — and even more so if deviations from the SM predictions would be discovered.

2.2 SUSY Higgs bosons

In supersymmetric theories the Higgs sector must be extended to at least two iso-doublet fields so that five or more physical Higgs particles are predicted. In the minimal extension the mass of the lightest neutral scalar Higgs particle h^0 is bounded from above to about 140 GeV, while the masses of the heavy neutral scalar and pseudoscalar Higgs bosons, H^0 and A^0, as well as the pair of charged Higgs bosons, $H^{\pm}$, may range from the electroweak scale to the (multi-)TeV region. The four heavy Higgs bosons tend to be nearly mass-degenerate.

The upper bound on the lightest Higgs mass is relaxed to about 200 GeV in more general scenarios if the fields remain weakly interacting up to the Planck scale as naturally assumed in supersymmetric theories.

Minimal supersymmetric theory

While search and study of the light h^0 Higgs boson follows the pattern summarized above for the SM Higgs boson in most of the parameter space, the heavy scalar and pseudoscalar Higgs bosons are produced in mixed pairs, in the same way as the charged Higgs bosons:

$$e^+e^- \to H^0A^0 \;\text{ and }\; H^+H^- \,. \tag{4}$$

For masses of the heavy Higgs bosons beyond about 200 GeV they cannot be detected at LHC in a wedge in $M_A/\tan\beta$ parameter space that is centered around the medium mixing angle $\tan\beta \sim 7$ and opens up to high Higgs masses. The wedge can be covered by pair production in e^+e^- collisions for masses $M_{H,A} \leq \sqrt{s}/2$, i.e., up to 500 GeV in the TeV phase of the machine. However, beyond this range, single production in photon-photon collisions,

$$\gamma\gamma \to H^0 \;\text{ and }\; A^0 \tag{5}$$

can cover the wedge up to Higgs masses of 800 GeV if a fraction of 80% of the total e^+e^- energy is transferred to the $\gamma\gamma$ system by Compton back-scattering of laser light [27]. Thus, a $\gamma\gamma$ collider may be the only facility in which, beyond the SM-type light Higgs boson, heavy Higgs bosons may be discovered before a multi-TeV linear collider can be operated. It is demonstrated in Fig. 4 how well the Higgs bosons can be detected in the two collider modes.

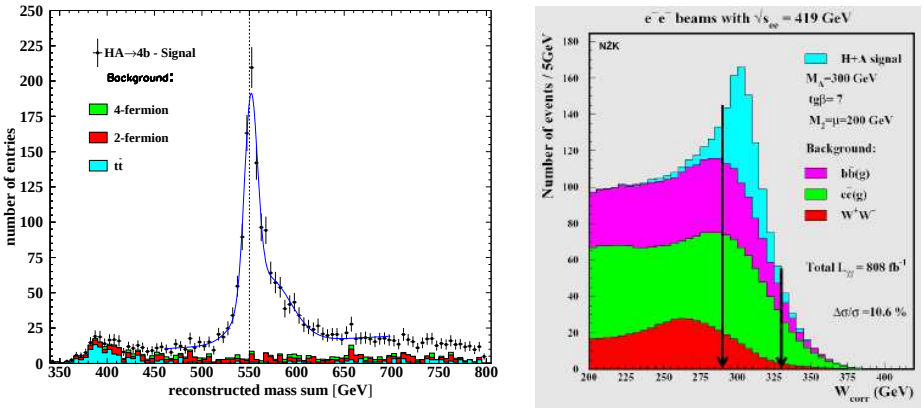

Figure 4: Left: Pair production of MSSM Higgs bosons HA in e^+e^- collisions; Ref. [28]; Right: Single Higgs production H and A in $\gamma\gamma$ fusion at a photon collider; Ref. [29].

High-precision measurements of the light Higgs mass can be exploited to determine parameters in the theory which are difficult to measure otherwise. By evaluating quantum corrections, the trilinear coupling A_t, for example, may be calculated from the Higgs mass,

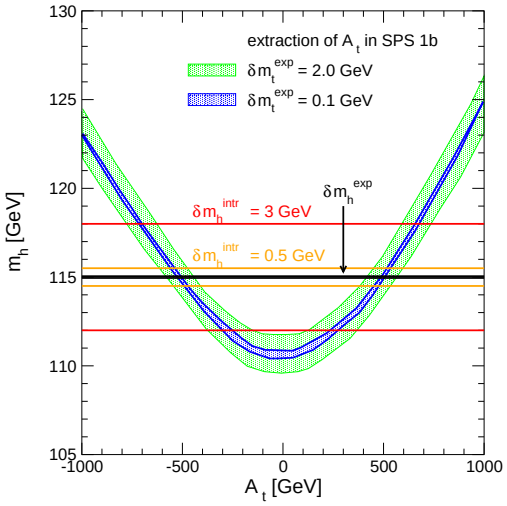

Figure 5: Extracting the trilinear coupling A_t from radiative corrections to the light MSSM Higgs mass; Ref. [30].

Fig. 5. For an error on the top mass of $\delta m_t = 100$ MeV, cf. Ref. [31], and an error on the Higgs mass of $\delta m_h = 50$ MeV, cf. Ref. [16], A_t can be determined at an accuracy of about 10%.

Extended supersymmetric theories

A large variety of theories, grand unified theories, string theories, etc., suggest additional Higgs fields beyond the minimal set in supersymmetric theories. Adding a complex iso-scalar to the iso-doublets, an additional pair of scalar and pseudoscalar Higgs particles is predicted. The axion-type character of the pseudoscalar boson renders this particle preferentially light. In general, the standard set of light and heavy Higgs bosons is expected in analogy to the MSSM, augmented however by a light scalar and a pseudoscalar Higgs boson, cf. Ref. [32], as illustrated in Fig. 6.

If the light pseudoscalar Higgs boson decays to b-quarks, a fan of b-jets is expected in Higgs-strahlung as the scalar Higgs bosons may decay to a pair of light pseudoscalar Higgs bosons, generating at least four b's in the final state [33, 34]. Nevertheless, a no-lose theorem for discovering at least one Higgs boson has been established for ILC while the situation is presently less clear for LHC.

2.3 Strong electroweak symmetry breaking

Within the Standard Model and its supersymmetric extensions, the Higgs field is introduced as a fundamental degree of freedom. Dynamical electroweak symmetry breaking is rooted in new strong interactions, not necessarily involving a Higgs boson. If global symmetries of these interactions are broken spontaneously, a set of Goldstone bosons will be generated, such as pions after breaking chiral symmetries in QCD. By absorbing these Goldstone bosons,

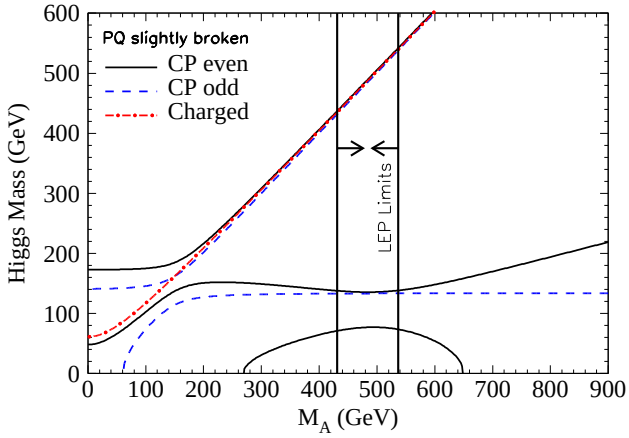

Figure 6: Typical Higgs mass spectrum in the non-minimal supersymmetric model NMSSM; Ref. [32].

longitudinal degrees of freedom and masses are generated for gauge bosons. Several scenarios have been developed along this path quite early [6, 35] as an alternative to the standard Higgs mechanism and more recently in a variant responding to the success of the light Higgs picture in accounting for the high-precision data in the electroweak sector.

Little-Higgs models

These models [36] are based on new unspecified interactions that are characterized by a scale Λ of order 10 TeV or more. The breaking of a huge global symmetry, e.g., SU(5) $\to$ SO(5), generates a set of [pseudo-]Goldstone bosons with properties characterized by the scale $F \sim \Lambda/4\pi$ which is close to a TeV. Collective breaking of the global symmetry retains a light mass at the level of $F/4\pi \sim v$ for some of the pseudo-Goldstone bosons, providing candidates for the SM-type Higgs boson.

While the new (multi-)TeV scalars and vectors may be searched for at LHC, at ILC their properties can be determined very precisely even if they remain virtual at the available energies [37, 38], cf. Fig. 7. Moreover, the entire parameter range of the model, as expected on general grounds, can be covered in searching for deviations from the Standard Model predictions in processes such as $e^+e^- \to f\bar{f}$, W^+W^-, ZH, and $\gamma\gamma \to H$.

Little-Higgs models predict a rich spectrum of new particles not only at the TeV scale, but new states may also be realized at low scales. Axion-type pseudoscalar bosons may be associated with the spontaneous breaking of $U(1)$ factors in the extra global symmetries. These particles have properties analogous to Higgs bosons [39]. They are produced parallel to Higgs bosons and their decay modes may be b-jet pairs:

$$e^+e^- \to t\bar{t}\eta \;\text{ with }\; \eta \to b\bar{b}\,. \tag{6}$$

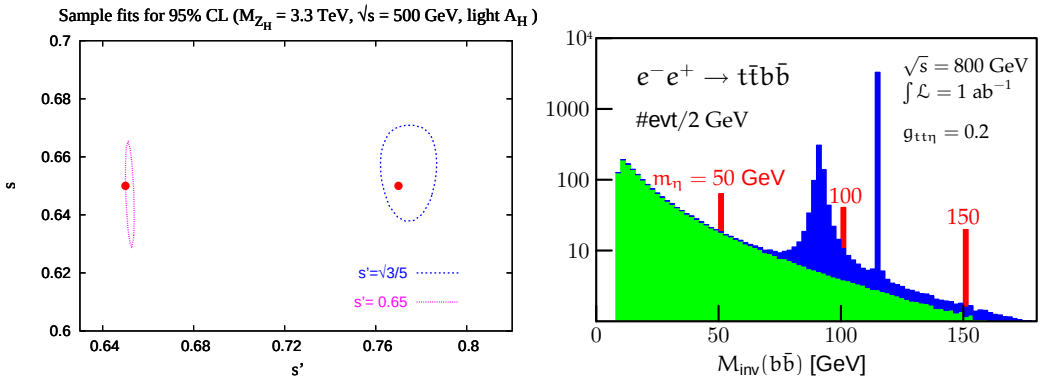

Figure 7: Little-Higgs models. Left: Sensitivity of SM processes to LH parameters; Ref. [38]. Right: Higgs and pseudoscalar boson production; Ref. [39].

Thus, instead of one Higgs resonance peak in the invariant $b\bar{b}$ mass in addition to the Z resonance, two peaks would be observed experimentally, Fig. 7. In $\gamma\gamma$ collisions the two states could be disentangled by using linearly polarized photon beams; scalars are generated in collisions of photons with parallel, pseudoscalars with perpendicular polarization vectors.

Strongly interacting W, Z bosons

If no Higgs boson will be observed with mass below 1 TeV, quantum-mechanical unitarity demands strong interactions between the electroweak gauge bosons, becoming effective at energies $(4\sqrt{2}\pi/G_F)^{1/2} \simeq 1.2$ TeV to damp the growth of the amplitudes for (quasi-)elastic WW scattering processes. To achieve compatibility with the S, T parameters extracted from the precision electroweak data at low energies, the underlying theory must deviate from the QCD template as a strongly-interacting theory.

The new interactions between the electroweak bosons, generically called W, can be expanded in a series of effective interaction terms with rising dimensions [40]. Scattering amplitudes are expanded correspondingly in a series characterized by the energy coefficients s/Λ_*^2. Demanding CP-invariance and isospin-invariance, as suggested by the value of the ρ parameter very close to one, two new dimension-4 interaction terms must be included in the expansion, $\mathcal{L}_4 = \alpha_4 \langle W_\mu W_\mu \rangle^2$ and $\mathcal{L}_5 = \alpha_5 \langle W_\mu W_\nu \rangle^2$, with coefficients $\alpha_{4,5} = v^2/\Lambda_{*4,5}^2$ expressed in the new strong interaction scales Λ_*, cf. Ref. [41]. To compensate the growth of the scattering amplitudes in the perturbative expansion, the new contributions must match the perturbative loop factor $1/16\pi^2$, i.e., the scale parameters are bounded from above by the value $4\pi v$.

Quasi-elastic WW scattering,

$$WW \to WW \quad \text{and} \quad ZZ \tag{7}$$

can be measured in the processes $e^+e^- \to \bar{\nu}\nu\, WW$ and $\bar{\nu}\nu ZZ$. The new interaction terms affect the total cross sections and the final-state distributions [41]. The reconstruction and separation of W and Z bosons in these analyses is a necessary condition, which can be

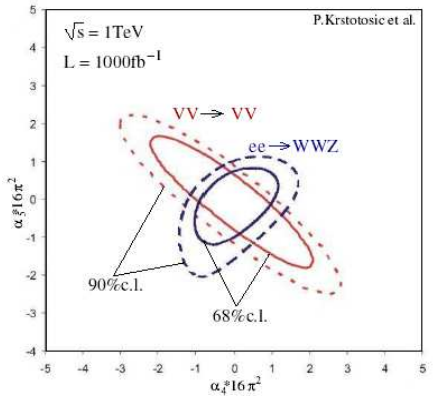

Figure 8: Measurement of parameters in new strong interactions of electroweak W bosons; Ref. [43].

fulfilled indeed in the clean environment of a lepton collider [42, 43]. Since the impact of the new interactions grows with the energy, ILC in the 1 TeV phase provides the most sensitive instrument for these studies. In fact, cf. Fig. 8, the entire range of Λ_* values can be covered experimentally:

$$\Lambda_* \leq 4\pi v \simeq 3\,\mathrm{TeV}\,. \tag{8}$$

The Λ_* values determine the masses of the resonances associated with the new interactions. The predictions can be helpful in the search for these resonances at LHC.

2.4 Extra space dimensions

A plethora of models have been constructed which can break the electroweak symmetries in scenarios of extra space dimensions. We will focus on a few characteristic aspects.

(i) In Randall-Sundrum models, a scalar *radion* field is introduced to stabilize the distance between the SM and the gravity brane. Carrying the same quantum numbers as the Higgs field, these two fields can mix and the properties of the Higgs boson will be altered [44]. In particular the branching ratio for Higgs decays to gluon jets may increase dramatically due to dominating radion decays to gluons, cf. [45].

(ii) Kaluza-Klein states can affect the $\gamma\gamma$ coupling and other loop-induced couplings of the Higgs field. Since the $\gamma\gamma$ width of the Higgs particle can be determined with an accuracy of 2% in the $\gamma\gamma$ fusion process at a photon-photon collider, the measurement provides the opportunity to study the particle sector associated with universal extra dimensions, for example, cf. Ref. [46].

(iii) Without introducing a scalar Higgs field, electroweak symmetries can be broken by choosing appropriate *boundary conditions* for the gauge fields in the compactified fifth dimension, with the fifth components of the gauge fields transformed to the longitudinal components of the massive gauge fields in $D = 4$ space-time dimensions. Cancellations which delay unitarity violations at high energies in WW scattering, are achieved by the exchange of Kaluza-Klein fields [47]. Sum rules connect the quartic couplings of the gauge fields with the couplings between gauge fields and Kaluza-Klein fields. The Kaluza-Klein

states can be searched for at LHC and ILC [48]. At ILC the couplings are expected to be measured, even for the exchange of virtual Kaluza-Klein fields, quite accurately.

3 Supersymmetry and unification

If supersymmetry is realized in nature, cf. Ref. [49], this fundamental symmetry will have an impact across all areas in microscopic physics and cosmology. In the Higgs sector, supersymmetry would be crucial for generating a light Higgs boson and stabilizing the electroweak scale in the background of the grand unification and Planck scales. The contribution of the supersymmetric particle spectrum to the evolution is essential for the electromagnetic, weak and strong gauge couplings to approach each other at a high scale, a necessary condition for the unification of all three gauge interactions. In addition, local supersymmetry provides a rationale for gravity by demanding the existence of spin-2 gravitons.

No firm prediction is possible for the mass scale of supersymmetry. However, for moderate values of the Higgs mixing parameter $\tan\beta$ a fairly low mass spectrum is indicated in the constrained minimal supersymmetric model by combining results from radiative corrections to electroweak precision observables, $(g_\mu - 2)/2$ and $b \to s\gamma$, with the measurement of the cold dark matter density at WMAP, cf. Fig. 9. The spectrum corresponding to a parameter set with close to maximal probability is depicted in Fig. 9. This spectrum had been chosen as a benchmark set SPS1a′ for a minimal supergravity scenario in the SPA project [51]. For the large $\tan\beta$ range, the typical mass scale shifts to somewhat larger values but, when

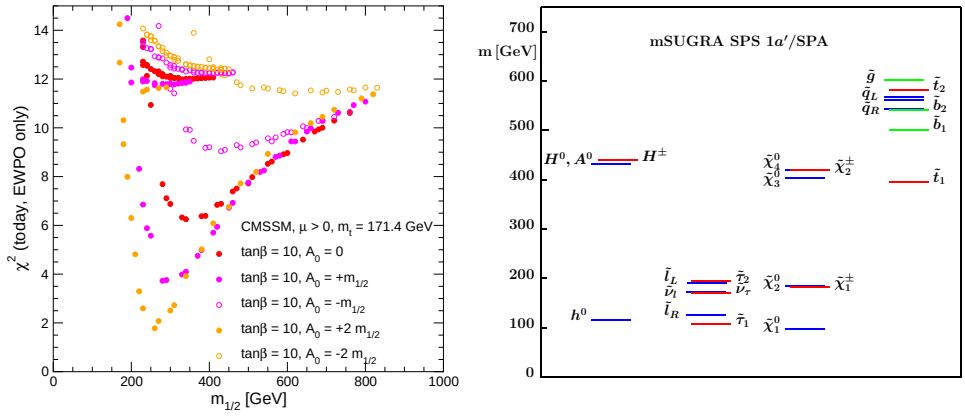

Figure 9: Left: Probability distribution of supersymmetry parameters (CMSSM/mSUGRA) from precision data for $\tan\beta = 10$; Ref. [50]. Right: The corresponding mass spectrum near the maximum, encoded in the benchmark point SPS1a′; Ref. [51].

using the approach of Ref. [50], the quality of the fit is worse.

The hadron collider LHC and an e^+e^- linear collider are a perfect tandem for exploring supersymmetry, cf. Ref. [52]. The heavy colored supersymmetric particles, squarks and gluinos, can be discovered for masses up to 3 TeV with large rates at LHC. Subsequent cascade decays give access to lower mass particles. The properties of the potentially lighter non-colored particles, charginos/neutralinos and sleptons, can be studied very precisely at

an e^+e^- linear collider by exploiting in particular polarization phenomena at such a facility. After the properties of the light particles are determined precisely, the heavier particles can subsequently be studied in the cascade decays with similar precision.

Coherent hadron and lepton analyses will provide a comprehensive and high-precision picture of supersymmetry at the electroweak scale, cf. Refs. [53, 54]. Moreover, the emerging picture defines, on one side, a solid basis for the reconstruction of the fundamental supersymmetric theory near the Planck scale, and for the connection of particle physics with cosmology on the other side.

3.1 Properties of supersymmetric particles

For illustration the parameters of the mSUGRA reference point SPS1a′ [51], a derivative of the Snowmass point SPS1a [55], will be adopted. This point gives a comprehensive picture of the potential which is offered by coherent analyses at high energy hadron and e^+e^- colliders. It is characterized by the following values of the soft parameters at the grand unification scale:

$$\begin{array}{ll} M_{1/2} = 250 \text{ GeV} & M_0 = 70 \text{ GeV} \\ A_0 = -300 \text{ GeV} & \text{sign}(\mu) = + \\ \tan\beta = 10 & \end{array} \tag{9}$$

The universal gaugino mass is denoted by $M_{1/2}$, the scalar mass by M_0 and the trilinear coupling by A_0; the sign of the higgsino mass parameter μ is chosen positive and $\tan\beta$, the ratio of the vacuum-expectation values of the two Higgs fields, in the medium range. The modulus of the higgsino mass parameter is fixed by requiring radiative electroweak symmetry breaking so that $\mu = +396$ GeV. As shown by the supersymmetric particle spectrum in Fig. 9, the squarks and gluinos can be studied very well at the LHC while the non-colored gauginos and sleptons can be analyzed partly at LHC and in comprehensive and precise form at an e^+e^- linear collider operating at a total energy up to 1 TeV.

Masses

At LHC, the masses can best be obtained by analyzing edge effects in the cascade decay spectra, cf. Ref. [56]. The basic starting point is the identification of a sequence of two-body decays: $\tilde{q}_L \to \tilde{\chi}_2^0 q \to \tilde{\ell}_R \ell q \to \tilde{\chi}_1^0 \ell\ell q$. The kinematic edges and thresholds predicted in the invariant mass distributions of the two leptons and the jet determine the masses in a model-independent way. The four sparticle masses [$\tilde{q}_L$, $\tilde{\chi}_2^0$, $\tilde{\ell}_R$ and $\tilde{\chi}_1^0$] are used subsequently as input for additional decay chains like $\tilde{g} \to \tilde{b}_1 b \to \tilde{\chi}_2^0 bb$, and the shorter chains $\tilde{q}_R \to q\tilde{\chi}_1^0$ and $\tilde{\chi}_4^0 \to \tilde{\ell}\ell$, which all require the knowledge of the sparticle masses downstream of the cascades. Residual ambiguities and the strong correlations between the heavier masses and the LSP mass are resolved by adding the results from ILC measurements which improve the picture significantly.

At ILC, very precise mass values can be extracted from threshold scans and decay spectra. The excitation curves for chargino $\tilde{\chi}_{1,2}^{\pm}$ production in S-waves rise steeply with the velocity of the particles near the thresholds,

$$\sigma \sim \sqrt{s - (\tilde{M}_i + \tilde{M}_j)^2} \tag{10}$$

and they are thus very sensitive to their mass values. The same holds true for mixed-chiral selectron pairs in $e^+e^- \to \tilde{e}_R^+\tilde{e}_L^-$ and for diagonal pairs in $e^-e^- \to \tilde{e}_R^-\tilde{e}_R^-$, $\tilde{e}_L^-\tilde{e}_L^-$ collisions, cf. Fig. 10. Other sfermions, as well as neutralinos, are produced generally in P-waves, with

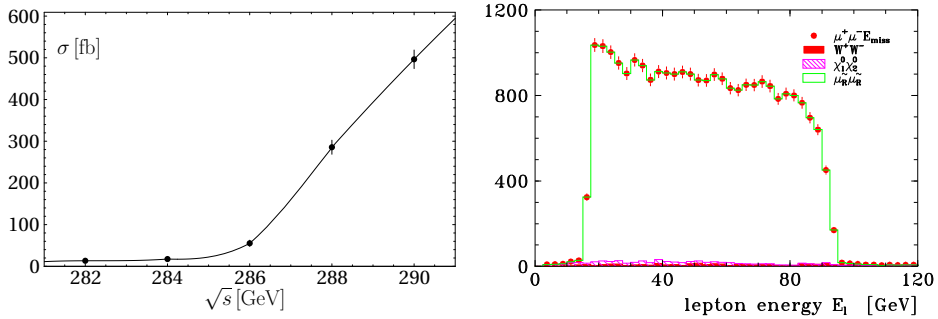

Figure 10: Left: Mass measurement in selectron $\tilde{e}^-\tilde{e}^-$ pair production; Ref. [57]; Right: Smuon and neutralino edges in smuon decays; Ref. [58].

a less steep threshold behavior proportional to the third power of the velocity. Additional information, in particular on the lightest neutralino $\tilde{\chi}_1^0$, can be obtained from the sharp edges of 2-body decay spectra, such as $\tilde{l}_R^- \to l^-\tilde{\chi}_1^0$. Denoting maximum and minimum edge of the decay lepton spectrum by $E_\pm$, cf. Fig. 10, slepton and $\tilde{\chi}_1^0$ masses can be derived from

$$\begin{aligned} m_{\tilde{\ell}} &= \sqrt{s}\,[E_+E_-]^{\frac{1}{2}}/(E_+ + E_-) \\ m_{\tilde{\chi}_1^0} &= m_{\tilde{\ell}}\,[1 - 2(E_+ + E_-)/\sqrt{s}]^{\frac{1}{2}} \end{aligned} \tag{11}$$

The accuracy in the measurement of the LSP $\tilde{\chi}_1^0$ mass can be improved at ILC by two orders of magnitude compared with LHC.

The values of typical mass parameters and their related measurement errors are presented in Tab. 1: "LHC" from LHC analyses and "ILC" from ILC analyses; the third column "LHC+ILC" presents the corresponding errors if the experimental analyses are performed coherently, i.e., the light particle spectrum, studied at ILC with high precision, is used as input set for the LHC analysis.

Spins

Determining the spin of new particles is an important measurement to clarify the nature of the particles and the underlying theory. This is necessary to discriminate the supersymmetric interpretation of new particles from other models. A well-known example is the distinction between supersymmetric theories and theories of universal extra space dimensions in which new Kaluza-Klein states carry spins different from supersymmetric particles.

The measurement of spins in particle cascades at LHC is an experimental challenge [59]. Spin measurements of sfermions at ILC, on the other hand, are quite easy. The polar angular distribution of smuon pairs, for example, approaches the characteristic $\sin^2\theta$ law for energies sufficiently above threshold. The smuons can be reconstructed up to a discrete ambiguity;

Particle	Mass	"LHC"	"ILC"	"LHC+ILC"
h^0	116.9	0.25	0.05	0.05
H^0	425.0		1.5	1.5
$\tilde{\chi}_1^0$	97.7	4.8	0.05	0.05
$\tilde{\chi}_2^0$	183.9	4.7	1.2	0.08
$\tilde{\chi}_4^0$	413.9	5.1	$3-5$	2.5
$\tilde{\chi}_1^\pm$	183.7		0.55	0.55
$\tilde{e}_R$	125.3	4.8	0.05	0.05
$\tilde{e}_L$	189.9	5.0	0.18	0.18
$\tilde{\tau}_1$	107.9	$5-8$	0.24	0.24
$\tilde{q}_R$	547.2	$7-12$	–	$5-11$
$\tilde{q}_L$	564.7	8.7	–	4.9
$\tilde{t}_1$	366.5		1.9	1.9
$\tilde{b}_1$	506.3	7.5	–	5.7
$\tilde{g}$	607.1	8.0	–	6.5

Table 1: Accuracies for representative mass measurements of SUSY particles in individual LHC, ILC and coherent "LHC+ILC" analyses for the reference point SPS1a′ [masses in GeV]. $\tilde{q}_R$ and $\tilde{q}_L$ represent the flavors $q = u, d, c, s$; cf. Ref. [53].

false solutions in the reconstruction generate a flat background underneath the signal [60]. By contrast, the determination of $spin = 1/2$ for charginos and neutralinos requires the analysis of angular final-state distributions [60].

Mixings

Mixing parameters must be extracted from measurements of cross sections and polarization asymmetries. In the production of charginos and neutralinos, both diagonal or mixed pairs can be exploited: $e^+e^- \to \tilde{\chi}_i^+\tilde{\chi}_j^-$ [i,j = 1,2] and $\tilde{\chi}_i^0\tilde{\chi}_j^0$ [i,j = 1,...,4]. The production cross sections for charginos are binomials in $\cos 2\phi_{L,R}$, the mixing angles rotating current to mass eigenstates. Using polarized electron and positron beams, the mixings can be determined in a model-independent way [61, 62].

The same methods can be applied to determine the mixings in the sfermion sector. The production cross sections for stop particle pairs, $e^+e^- \to \tilde{t}_i\tilde{t}_j^c$ [i,j = 1,2], depend on the mixing parameters $\cos/\sin 2\theta_{\tilde{t}}$ which can be determined with high accuracy by making use of polarized electron beams [63].

The measurement of the discrete quantum numbers of sfermions is another basic process. Using polarized electron and positron beams, the L/R quantum numbers of scalar electrons and positrons can be identified unambiguously even if the masses are nearly degenerate [12].

Couplings

Supersymmetry predicts the identity of Yukawa and gauge couplings among particle partners, in generic notation,

$$F\tilde{F}\tilde{V} = FFV \tag{12}$$

for gauge bosons V and gauginos $\tilde{V}$, and for fermions F and their scalar partners $\tilde{F}$. These fundamental relations can be studied experimentally in pair production of charginos and neutralinos which is partly mediated by the exchange of sneutrinos and selectrons in the t-channel, as well as selectron and sneutrino pair production which is partly mediated by neutralino and chargino t-channel exchanges.

An example is presented in Fig. 11 for the sensitivity which can be achieved at ILC in testing the identity of Yukawa and gauge couplings in selectron pair production. The

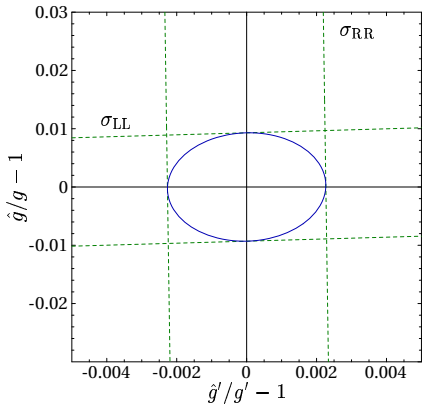

Figure 11: Relating the SU(2) and U(1) $\ell\tilde{\ell}\tilde{V}$ Yukawa couplings experimentally to the corresponding gauge couplings $\ell\ell V$ in selectron pair production; Ref. [57].

separation of the electroweak SU(2) and U(1) couplings is possible if polarized electron beams are available. At the end of course an overall analysis is required which takes into account the measurements of the masses and gaugino/higgsino mixing parameters of the neutralinos exchanged in the t-channel.

Same-sign dilepton production can be exploited at LHC to measure the identity $q\tilde{q}\tilde{g} = qqg$ for super-QCD Yukawa couplings [64]. Model-independent measurements of the couplings can be approached by making use of decay branching ratios determined in linear collider experiments.

3.2 Fundamental supersymmetric theory

The measurements described in the previous section provide the initial values for the evolution of the gauge couplings and the soft SUSY breaking parameters in the Lagrangian to the grand unification scale, cf. Ref. [65], where in many scenarios the fundamental supersymmetric theory is defined. The values at the electroweak scale are connected to the fundamental parameters at the GUT scale M_U by the renormalization group equations; to leading order,

$$
\begin{array}{ll}
\text{gauge couplings} & : \alpha_i = Z_i\,\alpha_U \\
\text{gaugino masses} & : M_i = Z_i\,M_{1/2} \\
\text{scalar masses} & : M^2_{\tilde{j}} = M_0^2 + c_j M^2_{1/2} + \sum_{\beta=1}^{2} c'_{j\beta}\Delta M^2_\beta \\
\text{trilinear couplings} & : A_k = d_k A_0 + d'_k M_{1/2}
\end{array}
$$

	Present/"LHC"	GigaZ/"LHC+ILC"
M_U	$(2.36 \pm 0.06) \cdot 10^{16}$ GeV	$(2.360 \pm 0.016) \cdot 10^{16}$ GeV
α_U^{-1}	24.19 ± 0.10	24.19 ± 0.05
$\alpha_3^{-1} - \alpha_U^{-1}$	0.97 ± 0.45	0.95 ± 0.12

Table 2: Precision in extracting the unified gauge coupling α_U, derived from the meeting point of α_1 with α_2, and the strong coupling α_3 at the GUT scale M_U. The columns demonstrate the results for the expected precision from LEP and LHC data, as well as the improvement due to a GigaZ linear collider analysis, cf. Ref. [53].

The index i runs over the gauge groups $i = \mathrm{SU}(3), \mathrm{SU}(2), \mathrm{U}(1)$. To this order, the gauge couplings, and the gaugino and scalar mass parameters of soft supersymmetry breaking depend on the Z transporters $Z_i^{-1} = 1 + b_i \alpha_U/(4\pi) \log(M_U^2/M_Z^2)$. The scalar mass parameters $M_{\tilde{j}}^2$ depend also on the Yukawa couplings. Beyond these approximate solutions, the evolution equations have been solved numerically.

Gauge coupling unification

Measurements of the gauge couplings at the electroweak scale strongly support the unification of the couplings [66] at a scale $M_U \simeq 2 \times 10^{16}$ GeV, with a precision at the per-cent level. The couplings do not meet exactly, cf. Fig. 12 and Tab. 2, most evident after taking into

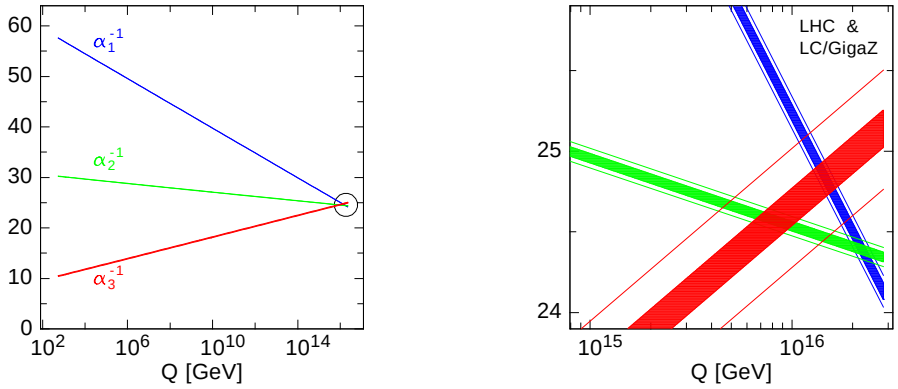

Figure 12: Gauge coupling unification at GigaZ; Ref. [53].

account results from GigaZ runs. The differences are to be attributed to threshold effects at the unification scale M_U. The quantitative evaluation implies important constraints on the particle content of the physics scenario in the grand unification / Planck region.

Gaugino and scalar mass parameters

The results for the evolution of the mass parameters from the electroweak scale to the GUT scale M_U are shown in Fig. 13. On the left of Fig. 13 the evolution is presented for

the gaugino parameters M_i^{-1}. The model-independent reconstruction of the fundamental

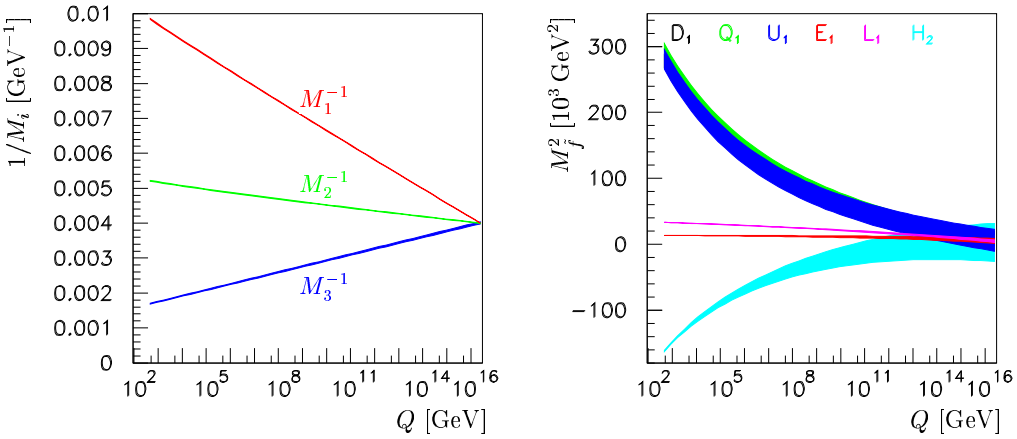

Figure 13: Unification of gaugino and scalar mass parameters; Ref. [53].

parameters and the test of universality in the SU(3)×SU(2)×U(1) group space are clearly under excellent control.

In the same way the evolution of the scalar mass parameters can be studied, presented on the right of Fig. 13 for the first/second generation. While the slepton parameters can be determined very precisely, the accuracy deteriorates for the squark parameters and the Higgs parameter $M_{H_2}^2$.

The evolution of the scalar mass parameters is quite distinct from scenarios in which supersymmetry is broken by a different mechanism. A typical example is gauge mediated supersymmetry breaking GMSB where regularities are predicted at an intermediate energy scale but extrapolations to Planck scale energies lead to markedly non-universal mass parameters [65]. Thus the microscopic picture of supersymmetry breaking can be explored this way experimentally.

These examples demonstrate that high-precision experiments at high-energy colliders allow us to reconstruct crucial elements of the physics scenario near the Planck scale. They shed light on a domain where in many theoretical approaches the roots of physics are located including gravity.

3.3 Left-right symmetric extension

The complex structure observed in the neutrino sector requires the extension of the minimal supersymmetric Standard Model MSSM, e.g., by a superfield including the right-handed neutrino field and its scalar partner. If the small neutrino masses are generated by the seesaw mechanism [67], a similar type of spectrum is induced in the scalar sneutrino sector, splitting into light TeV-scale and very heavy masses. The intermediate seesaw scales will affect the evolution of the soft mass terms which break the supersymmetry at the high (GUT) scale, particularly in the third generation with large Yukawa couplings. This will provide us with the opportunity to measure, indirectly, the intermediate seesaw scale of the

third generation [68].

The measurement of the seesaw scale can be illustrated in an SO(10) model [69] in which the Yukawa couplings in the neutrino sector are proportional to the up-type quark mass matrix. The masses of the physical right-handed Majorana neutrinos are hierarchical $\propto m_{\rm up}^2$, and the mass of the heaviest neutrino is roughly estimated by $M_{\rm R_3} \sim m_t^2/m_{\nu_3}$ which, for $m_{\nu_3} \sim 10^{-2}$ eV, amounts to $\sim 10^{15}$ GeV, i.e., a value close to the grand unification scale M_U.

Since the $\nu_{\rm R}$ is unfrozen only beyond $Q = M_{\nu_{\rm R}}$ the impact of the LR extension becomes visible in the evolution of the scalar mass parameters only at very high scales, but the effect of $\nu_{\rm R}$ can be manifest only in the third generation where the Yukawa coupling is large enough [65]. The evolution of the scalar mass parameters in the third generation and the Higgs mass parameter is sketched in Fig. 14. The kinks in the L3, H2 lines are induced by

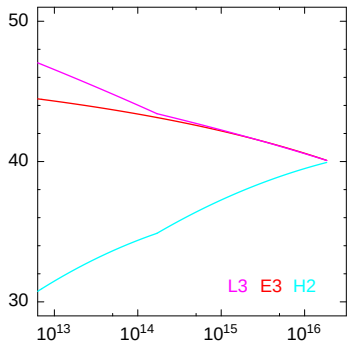

Figure 14: Impact of the heavy right-handed neutrino mass on the evolution of the scalar mass parameters in LR symmetric theories; Refs. [65, 68].

the right-handed neutrino. Only if $\nu_{\rm R}$, $\tilde{\nu}_{\rm R}$ are included, the picture is compatible with the assumption of universality.

The kinks in the evolution of $M^2_{\tilde{L}_3}$ shift the physical masses [squared] of the $\tilde{\tau}_{\rm L}$ and $\tilde{\nu}_{\tau{\rm L}}$ particles of the third generation by the amount $\Delta_\nu[M_{\rm R}]$ compared with the slepton masses of the first two generations. The measurement of

$$|m^2_{\tilde{\tau}} - m^2_{\tilde{e}}|/m^2_{\tilde{e}} \propto \log(M^2_{\rm GUT}/M^2_{\rm R_3}) \tag{13}$$

can be exploited to determine the neutrino seesaw scale of the third generation [70],

$$M_{\rm R_3} = 7.4^{+3.8}_{-2.8} \times 10^{14}{\rm GeV} \tag{14}$$

in the LR extended SPS1a′ scenario. Thus, the analysis provides us with a unique estimate of the high-scale $\nu_{\rm R}$ seesaw mass parameter $M_{\rm R_3}$.

3.4 Split Supersymmetry

For a successful unification of forces at the GUT scale the size of the sfermion mass scale M_0 is irrelevant, since each generation of sfermions incorporates a complete representation

of SU(5) [or SO(10)]. Likewise, the dark-matter prediction of the MSSM and its extensions does not rely on the value of M_0, but rather on the existence of a conserved discrete quantum number, R parity. These facts are compatible with the speculation that the sfermion mass scale may actually be much higher than the gaugino mass scale, effectively removing all scalar partners of the matter fields and the extra heavy Higgs states of the MSSM from the low-energy spectrum [71].

In such a scenario sources of flavor violation besides CKM mixing are naturally absent, removing the requirement of sfermion-mass degeneracy from the mechanism of supersymmetry breaking. On the other hand, the Higgs potential is fine-tuned as in the non-supersymmetric SM.

With a sufficiently high sfermion mass scale, e.g., $M_0 \sim 10^9$ GeV, the gluino acquires a macroscopic lifetime and, for the purpose of collider experiments, behaves like a massive, stable color-octet parton. This leads to characteristic signatures at LHC. Detection of such a particle is possible up to $m_{\tilde{g}} = 1 - 2$ TeV [72, 73]. The Higgs boson mass is expected to be above the conventional MSSM mass range. Due to the absence of cascade decays, the production of the non-colored gauginos and higgsinos at LHC proceeds only via electroweak annihilation processes, and the production rates are thus considerably suppressed compared to conventional MSSM scenarios.

In this situation, the analysis of chargino and neutralino pair-production at ILC provides the information necessary to deduce the supersymmetric nature of the model. Extracting the values of chargino/neutralino Yukawa couplings, responsible for the mixing of gaugino and higgsino states, reveals the anomalous effects induced by the splitting of the gaugino and sfermion mass scales [72]. Furthermore, these parameters determine the higgsino content of the LSP and thus the relic dark-matter density predicted by the Split Supersymmetry Model [74].

3.5 String effective theories

Heterotic string theories give rise to a set of 4-dimensional dilaton S and moduli T superfields after compactification. The vacuum expectation values of S and T, generated by genuinely non–perturbative effects, determine the soft supersymmetry breaking parameters.

The properties of the supersymmetric theories are quite different for dilaton and moduli dominated scenarios, quantified by the mixing angle θ. This angle θ characterizes the $\tilde{S}$ and $\tilde{T}$ components of the wave function of the Goldstino, which is associated with the breaking of supersymmetry. The mass scale is set by the second parameter of the theory, the gravitino mass $m_{3/2}$.

In leading order, the masses [75] are given by

$$M_i = -g_i^2 m_{3/2} \langle S \rangle \sqrt{3} \sin\theta + ... \quad (15)$$

$$M_j^2 = m_{3/2}^2 \left(1 + n_j \cos^2\theta\right) + ... \quad (16)$$

for the gaugino sector and the scalar sector, respectively. A dilaton dominated scenario, $\sin\theta \to 1$, leads to universal boundary conditions of the soft supersymmetry breaking parameters. On the other hand, in moduli dominated scenarios, $\cos\theta \to 1$, the gaugino mass parameters are universal, but universality is not realized for the scalar mass parameters. The breaking is characterized by integer modular weights n_j which quantify the couplings between the matter and the moduli fields. Within one generation significant differences between left and right field components and between sleptons and squarks can occur.

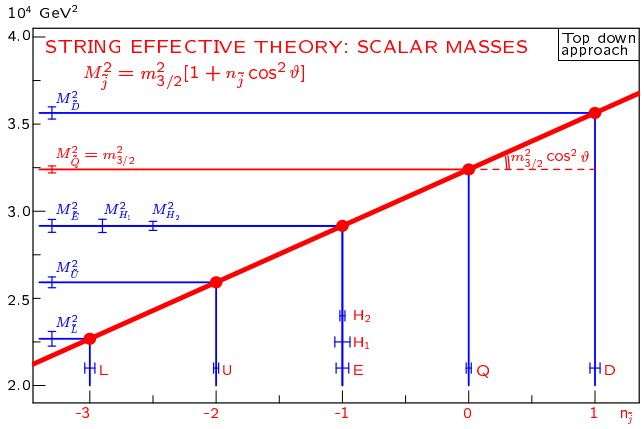

Figure 15: The linear relation between integer modular weights and scalar mass parameters in string effective theories; cf. Ref. [65].

The results [65] for the analysis of a mixed dilaton/moduli superstring scenario with dominating dilaton component, $\sin^2\theta = 0.9$, and with different couplings of the moduli field to the (L,R) sleptons, the (L,R) squarks and to the Higgs fields corresponding to the O–I representation $n_{L_i} = -3$, $n_{E_i} = -1$, $n_{H_1} = n_{H_2} = -1$, $n_{Q_i} = 0$, $n_{D_i} = 1$ and $n_{U_i} = -2$, are presented in Fig. 15. The gravitino mass is chosen to be 180 GeV in this analysis. Given this set of superstring induced parameters, the evolution of the gaugino and scalar mass parameters can be exploited to determine the modular weights n. Fig. 15 demonstrates how stringently this theory can be tested by analyzing the integer character of the entire set of modular weights.

Thus, high-precision measurements at high energy proton and lepton colliders may provide access to crucial derivative parameters in string theories.

3.6 Intermediate gauge bosons

Gauge bosons at the intermediate TeV scale are motivated by many theoretical approaches, cf. Ref. [76]. The breaking of GUT theories, based on SO(10) or E(6) symmetries for example, may leave one or several U(1) remnants unbroken down to TeV energies, before the symmetry is reduced finally to the SM symmetry:

$$\begin{aligned} \mathrm{SO}(10) &\rightarrow \mathrm{SM} \times \mathrm{U}(1) && (17) \\ \mathrm{E}(6) &\rightarrow \mathrm{SO}(10) \times \mathrm{U}(1) \rightarrow \mathrm{SM} \times \mathrm{U}(1) \times \mathrm{U}(1) \\ &\rightarrow \mathrm{SM} \times \mathrm{U}(1) && (18) \end{aligned}$$

The final U(1) remnant of E(6) is a linear combination χ, ψ or η of the U(1)'s generated in the two-step symmetry breaking mechanism.

Such intermediate gauge bosons can be searched for at LHC for masses up to about 5 TeV. The role of ILC is twofold. First, by analyzing the effect of virtual Z' s-channel exchange on the cross sections and angular distributions of fermion pair production, $e^+e^- \rightarrow f\bar{f}$, the

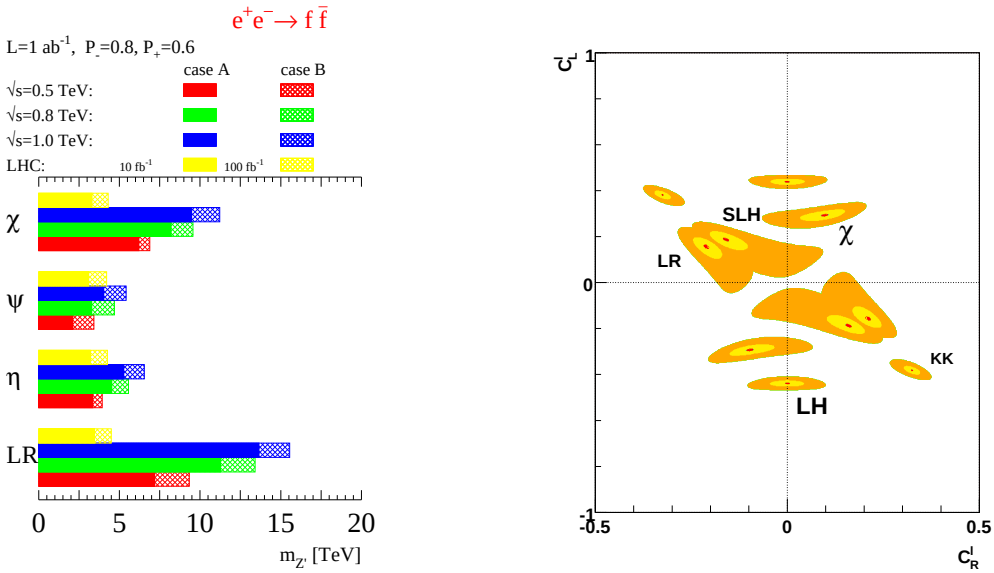

Figure 16: Z′ masses [77], and couplings [78], in extended SO(10), E(6) gauge theories.

sensitivity to new gauge boson scales can be extended significantly, cf. Fig. 16, in SO(10) LR symmetric theories up to $\simeq$ 15 TeV at ILC (and up to $\simeq$ 35 TeV at CLIC [79]). Second, the couplings of the new Z' boson to SM fermions can be determined very precisely, Fig. 16. The various models can obviously be discriminated quite clearly and the nature of the underlying gauge symmetry can be identified.

4 Extra space dimensions

A large variety of models have been developed in which the ordinary 4-dimensional space-time is extended to higher dimensions already at energies of order 1 TeV. The ILC potential in analyzing such models, in which the extra dimensions are compactified at low scales, will be illustrated in two examples.

ADD scenario

In the ADD scenario [10] gravity extends from the brane on which the fields of the Standard Model are located, to the higher D $= 4 + \delta$ dimensions. It becomes strong in the extended space already at the fundamental Planck scale $\Lambda_{\rm D}$ of order TeV, much below the effective standard Planck scale $\Lambda_{\rm Pl}$ of order 10^{19} GeV, and it appears weak only if projected onto the 4-dimensional SM brane. The radii of the compactified higher dimensions are related to the Planck scale by $\Lambda_{\rm Pl}^2 = R^\delta \Lambda_{\rm D}^{2+\delta}$. The associated Kaluza-Klein states with masses $\sim n/R$ densely populate a tower with energy spacings of a small fraction of eV up to a few MeV, depending on the number of extra space dimensions.

At e^+e^- linear colliders the two crucial parameters of the ADD model, the fundamental Planck scale $\Lambda_{\rm D}$ and the number δ of extra space dimensions, can be disentangled by varying the cm energy of the collider. The cross section for the process of single γ production,

$$e^+e^- \to \gamma + G_{\rm KK} \tag{19}$$

where $G_{\rm KK}$ denotes the sum over the invisible graviton states of the Kaluza-Klein tower, depends on these two parameters in the form [80]

$$\sigma(e^+e^- \to \gamma + \not{E}) = \frac{c_\delta}{\Lambda_{\rm D}^2}\left(\frac{\sqrt{s}}{\Lambda_{\rm D}}\right)^\delta . \tag{20}$$

Thus, the larger the number of extra dimensions the stronger would be the rise of the cross section for single isolated photons with the collider energy, Fig. 17.

RS scenario

While in the previous model space is flat in the standard and extra dimensions, it is curved in the RS(RS1) model [11]. The geometry is described by an exponential warp factor $\exp(-2kr_c\phi)$, characterized by the compactification radius r_c and the curvature k. The coordinate ϕ spans the distance between the gravity brane located at $\phi = 0$ and the SM brane located at $\phi = \pi$. Since the scale of physical processes on the SM brane is given by $\Lambda_{\rm SM} = \Lambda_{\rm Pl}\exp(-kr_c\pi) \sim 1$ TeV, the compactification radius r_c is estimated to be, roughly, one order of magnitude larger than the curvature radius k^{-1}, while k itself is of the order of the effective 4-dimensional Planck scale. The characteristics of our eigen-world on the 4-dimensional SM brane are described by the two parameters k and r_c, with the second parameter generally substituted by $\Lambda_{\rm SM}$.

The Kaluza-Klein tower of the gravitons on the SM brane is characteristically different from towers associated with flat spaces, the sequence of masses [82] given by

$$M_n = x_n\, k\, \exp(-kr_c\pi) = x_n \Lambda_{\rm SM}\, k\, /\Lambda_{\rm Pl} \tag{21}$$

where x_n are the roots of the first-order Bessel functions. Such states can be searched for in fermion pair production $e^+e^- \to \mu^+\mu^-$, affecting this process by resonant s-channel exchanges. Fixing the lowest KK state to a mass of 600 GeV, the sequence of KK excitations is displayed in Fig. 17. The width of the KK states depends on the curvature $k \sim \Lambda_{\rm Pl}$ in the fifth dimension. The cross sections turn out to be very large if the parameters are such that the lowest KK states can be generated at the collider as an s-channel resonance.

If in addition to the gravity field SM fields are expanded to the extra space dimension, constraints derived from the SM precision measurements shift the mass scale of the Kaluza-Klein towers to considerably large values in the multi-TeV range and only virtual effects could be observed in SM processes at a TeV collider.

5 Cosmology connection

Collider physics programs focus in connection with cosmology presently on two fundamental problems, cf. Ref. [83]:

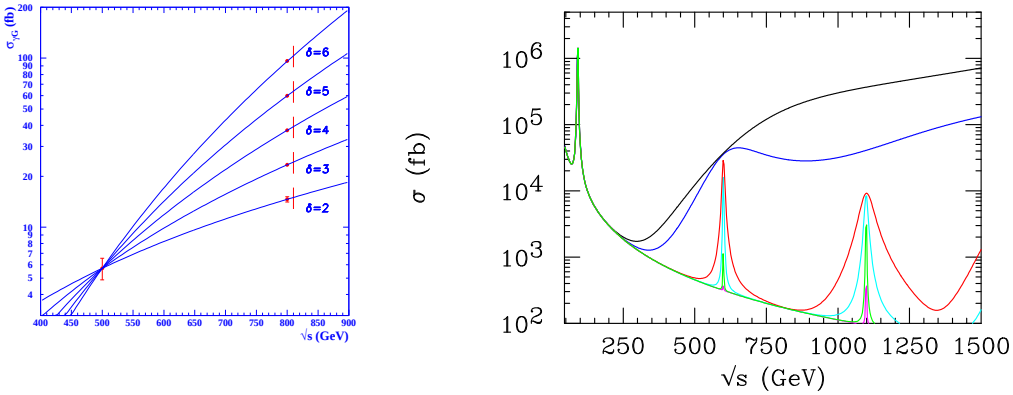

Figure 17: Left: Measuring the Planck scale and the number of dimensions in ADD scenarios; Ref. [81]. Right: Kaluza-Klein excitations in RS scenarios for various values of the curvature k; Ref. [82].

- the mechanism responsible for the baryon asymmetry: $\rho_{\mathrm{B}} =$ $4.0 \pm 0.4\%$
- the particle character of cold dark matter: $\rho_{\mathrm{CDM}} =$ $23 \pm 4\%$

These central problems of physics cannot be solved within the framework of the Standard Model. Various solutions have been worked out which require experiments at high energy colliders to establish the proposed mechanism for generating the baryon asymmetry in the universe and for clarifying the nature of cold dark matter. Even if a single particle species were the main component of cold dark matter in the universe, the theoretical origin will in general be so complex that laboratory experiments are required to achieve the proper understanding of this phenomenon.

5.1 Baryon asymmetry

Two approaches for generating the baryon asymmetry are widely discussed in the literature: baryogenesis mediated by leptogenesis, and electroweak baryogenesis based on the supersymmetric extension of the Standard Model.

Leptogenesis

If leptogenesis [84] is the origin of the observed baryon asymmetry, the roots of this phenomenon are located near the Planck scale. CP-violating decays of heavy right-handed Majorana neutrinos generate a lepton asymmetry which is transferred to the quark/baryon sector by sphaleron processes. Heavy neutrino mass scales as introduced in the seesaw mechanism for generating light neutrino masses and the size of the light neutrino masses needed for leptogenesis define a self-consistent frame which is compatible with all experimental observations [85].

As shown in the preceding chapter, in some SUSY models the size of the heavy seesaw scales can be related to the values of the charged and neutral slepton masses [68]. A sum rule relates the difference between the slepton masses of the first two and the third generation to the mass of the heavy right-handed Majorana neutrino in the third generation within SO(10) based supergravity theories. In this way the size of the seesaw scale can well be estimated.

Electroweak baryogenesis in supersymmetry

One of Sakharov's conditions for generating the baryon asymmetry of the universe requires a departure from thermal equilibrium. If triggered by sphaleron processes at the electroweak phase transition, the transition must be sufficiently strong of first order. Given the present bounds on the Higgs mass, this cannot be realized in the Standard Model. However, since top and stop fields modify the Higgs potential strongly through radiative corrections, supersymmetry scenarios can give rise to first-order transitions, cf. Ref. [86]. The parameter space of the MSSM is tightly constrained in this case: The mass of the light Higgs boson is bounded by 120 GeV from above, and the mass of the light stop quark is required to be smaller than the top quark mass, cf. Ref. [87].

This scenario suggests that the mass of the stop quark is only slightly larger than the lightest neutralino (LSP) mass. The correct density of cold dark matter is generated by stop-neutralino coannihilation in this region of parameter space, leading to tight constraints for the masses of the two particles.

While studies of the light stop quark are very difficult at hadron colliders if the main decay channel is the two-body decay $\tilde{t}_1 \to c\tilde{\chi}_1^0$ with a low-energy charm jet in the final state, the clean environment of an e^+e^- collider allows for precision studies of the system also in

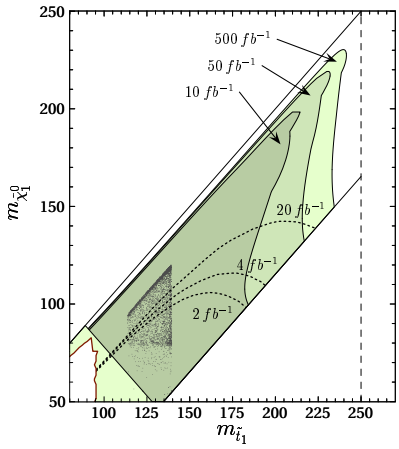

Figure 18: ILC coverage of stop/neutralino parameter space, dark grey points, in the MSSM based electroweak phase transition; Ref. [87].

such configurations. This is demonstrated in Fig. 18 which proves that a linear collider covers completely the region of dark gray points which are compatible with precision measurements

of the cold dark matter density.

5.2 Cold dark matter

Cold dark matter (CDM) is the dominant component of matter in the universe. So far it has not been possible yet to reveal its microscopic nature. Attempts to solve this problem form an intimate link between cosmology and particle physics. CDM may be a complex structure and a mixture of several components. Theoretical particle physics offers hypothetical particle candidates which could be discovered in the next generation of accelerators. After determining the properties of candidate particles in laboratory experiments, their density in the universe can be predicted and the prediction can be confronted with cosmological precision measurements. In addition, compatibility with direct and indirect search experiments must be checked. In this way a closed circle may evolve which provides a self-consistent picture of the nature of cold dark matter and its distribution in the universe.

Theories which provide a CDM candidate must have a conserved parity quantum number. Examples are R parity in supersymmetric models, KK parity in extra-dimensional models, or T parity in Little-Higgs theories. The lightest particle with odd parity is then stable, must be charge- and color-neutral, and thus provides a CDM candidate. If this particle is in or below the TeV mass range and interacts with matter, it will be seen via missing-energy signatures at LHC. At ILC, a precise determination of its mass and interactions is possible due to kinematical hermeticity and low background, independently of the embedding theory.

Among the candidate theories, two specific examples will be summarized briefly to illuminate the ILC potential in clarifying the nature of cold dark matter particles. The examples chosen are the supersymmetric extension of the Standard Model embedded in minimal supergravity in which the lightest neutralino is the cold dark matter particle, and a supergravity theory in which the gravitino is identified with this particle. In the first example, the characteristic are the mass scale with a value near the electroweak scale, and the weak interactions of CDM. In the second example, CDM interacts only through gravity.

Neutralino cold dark matter

In the mSUGRA parameter range four characteristic areas have been identified in which the observed relic density [88] can be accommodated, cf. Fig. 19, and they have recently been studied systematically [89]-[92].

(i) In the *bulk region* the gaugino mass parameter $M_{1/2}$ and the scalar mass parameter M_0 are both in the area surrounding the electroweak scale. Neutralino pairs annihilate into fermion pairs. This area, including the benchmark point SPS1a′, has been studied very thoroughly for LHC as well as ILC experiments. From the ILC studies the CDM density is expected to be determined within an accuracy of about 2%, thus matching the precision expected from measurements of the Planck satellite in the near future.

(ii) In the *focus point region* the gaugino mass parameter remains moderate but the scalar mass parameter is very large. While the spectrum of charginos and neutralinos appears accessible at ILC, sleptons can be produced, if at all, only at a multi-TeV collider. Split Supersymmetry, where sleptons are completely inaccessible, is an extreme case of this scenario. Neutralino pairs annihilate primarily to gauge bosons. The prediction of the relic density is strongly correlated with the mass difference between the lightest chargino and neutralino as demonstrated in Fig. 19.

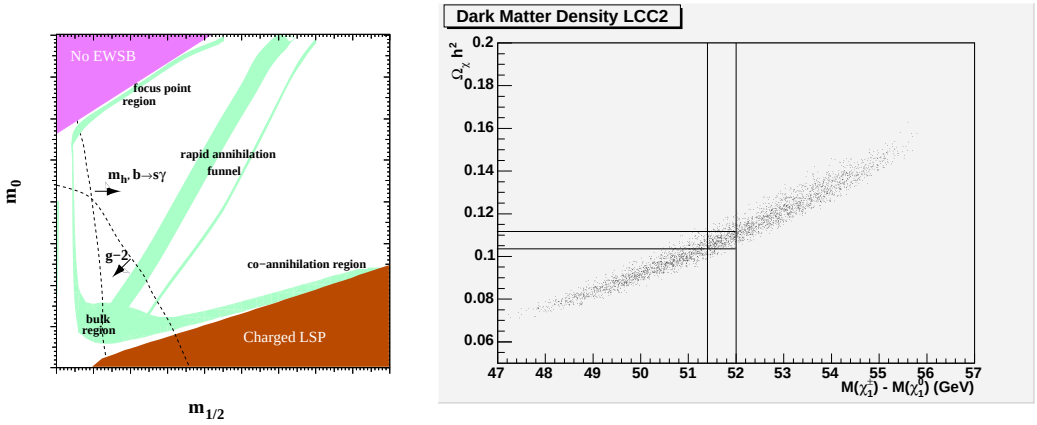

Figure 19: Left: Characteristics of mSUGRA parameter regions constrained by precision data on the relic density; cf. Ref. [83]. Right: Sensitivity of the prediction for the relic density from parameter measurements in the focus point region; Ref. [89], see also Refs. [90].

	character	channel	sensitivity	LHC	ILC
SPS1a′	bulk	$\tilde{\chi}\tilde{\chi} \to \tau\tau,\, bb$	$\tilde{\tau},\, \tilde{b}$	10%	2%
LCC2	focus point	$\tilde{\chi}\tilde{\chi} \to WW, ZZ$	$\tilde{V}\tilde{H}$ mix	82%	8%
LCC3	$\tilde{\tau}\tilde{\chi}$ co-ann.	$\tilde{\tau}\tilde{\chi} \to \tau\gamma$	$M[\tilde{\tau} - \tilde{\chi}_1^0]$	167%	18%
LCC4	A funnel	$\tilde{\chi}\tilde{\chi} \to A$	$M_A,\, \Gamma_A$	405%	19%

Table 3: Predictions of the relic density from measurements of supersymmetric particle properties at the LHC and the TeV linear collider; Ref. [92].

(iii) The $\tilde{\tau}\tilde{\chi}$ *coannihilation region* with moderate to large $M_{1/2}$ and moderate M_0 is difficult to explore experimentally as $\tilde{\tau} \to \tau\tilde{\chi}_1^0$ decays must be studied in which stau and neutralino are close in mass so that the visible τ in the final state carries only a small amount of energy and is hard to detect.

(iv) In the *funnel region* neutralino annihilation is mediated by an s-channel Higgs boson. Predictions of the relic density in this region depend on the properties of the pseudoscalar Higgs boson A, the mass M_A and the width Γ_A; errors of the predictions are correspondingly large.

The accuracy of the relic density is presently set by thw WMAP analysis to

$$\Omega h^2 = 0.104^{+0.007}_{-0.013} \tag{22}$$

The accuracy is expected to be improved by the PLANCK satellite to 1.4%. Choosing a representative point for each of the characteristic regions, the predicted errors for the prediction of the relic density are collected in Tab. 3. Evidently, the accuracy expected in the analysis at the TeV linear collider analysis significantly improves expectations for LHC.

Gravitino cold dark matter

In supergravity models the gravitino $\tilde{G}$ itself may be the lightest supersymmetric particle, building up the dominant CDM component, cf. Ref. [93]. In such a scenario, with a gravitino mass in the range of 100 GeV [in contrast to gauge-mediated supersymmetry breaking with very light gravitino mass], the lifetime of the next-to-lightest supersymmetric particle can become very long as the gravitino coupling is only of gravitational strength. The lifetime of the NLSP $\tilde{\tau}$ in the gravitino decay process,

$$\tau[\tilde{\tau} \to \tau + \tilde{G}] = const \times M_{\tilde{G}}^2 M_{\rm Pl}^2 / M_{\tilde{\tau}}^5 \,, \tag{23}$$

can extend to macroscopic scales [94], suggesting special experimental efforts to catch the long-lived $\tilde{\tau}$'s and to measure their lifetime [95]. Production in e^+e^- annihilation determines the $\tilde{\tau}$ mass, the observation of the τ energy in the $\tilde{\tau}$ decay the gravitino mass. The measurement of the lifetime can subsequently be exploited to confirm the Planck scale $M_{\rm Pl}$ as the scale of the fundamental supergravity coupling.

6 Summary

The ILC can contribute to solutions of key questions in physics,

- *Electroweak Symmetry Breaking*: The Higgs mechanism *sui generis* can be established for breaking the electroweak symmetries and generating the masses of the fundamental particles.
- *Grand and Ultimate Unification*: A comprehensive and high-resolution picture of supersymmetry can be drawn by coherent analyses of hadron and lepton collider experiments. Thus the colliders may become telescopes to the physics scenario near the Planck scale where particle physics is linked with gravity and where the basic roots of physics are expected to be located.
- *Extra Space Dimensions*: The parameters of an extended space-time picture can be determined, the fundamental Planck scale and the number of extra dimensions. New Kaluza-Klein states can either be generated directly or their effect on Standard Model processes can be explored.
- *Cosmology Connection*: Drawing a microscopic picture of particles building up cold dark matter, the basis necessary for the understanding of matter in the universe can be provided by collider experiments. In addition, crucial elements for explaining the baryon asymmetry in the universe can be reconstructed.

Collider experiments will thus be essential instruments for unraveling the fundamental laws of nature.

References

[1] Slides:
`http://ilcagenda.linearcollider.org/contributionDisplay.py?contribId=4&sessionId=0&confId=1296`

[2] J.A. Aguilar-Saavedra *et al.* [ECFA/DESY LC Physics Working Group Collaboration], arXiv:hep-ph/0106315; T. Abe *et al.* [American Linear Collider Working Group Collaboration], arXiv:hep-ex/0106055, hep-ex/0106056, hep-ex/0106057, and hep-ex/0106058; K. Abe *et al.* [ACFA Linear Collider Working Group Collaboration], arXiv:hep-ph/0109166.

[3] A. Djouadi, J. Lykken, K. Monig, Y. Okada, M. J. Oreglia and S. Yamashita, arXiv:0709.1893 [hep-ph].

[4] E. Accomando *et al.* [CLIC Physics Working Group Collaboration], arXiv:hep-ph/0412251.

[5] P. W. Higgs, Phys. Lett. **12** (1964) 132 and Phys. Rev. **145** (1966) 1156; F. Englert and R. Brout, Phys. Rev. Lett. **13** (1964) 321; G. S. Guralnik, C. R. Hagen and T. W. B. Kibble, Phys. Rev. Lett. **13** (1964) 585.

[6] S. Weinberg, Phys. Rev. D **13** (1976) 974 and Phys. Rev. D **19** (1979) 1277; L. Susskind, Phys. Rev. D **20** (1979) 2619.

[7] H. Georgi and S. L. Glashow, Phys. Rev. Lett. **32** (1974) 438; H. Georgi, H. R. Quinn and S. Weinberg, Phys. Rev. Lett. **33** (1974) 451.

[8] J. Wess and B. Zumino, Nucl. Phys. B **70** (1974) 39.

[9] I. Antoniadis and K. Benakli, Phys. Lett. B **326** (1994) 69 [arXiv:hep-th/9310151].

[10] N. Arkani-Hamed, S. Dimopoulos and G. R. Dvali, Phys. Rev. D **59** (1999) 086004 [arXiv:hep-ph/9807344].

[11] L. Randall and R. Sundrum, Phys. Rev. Lett. **83** (1999) 4690 [arXiv:hep-th/9906064].

[12] G. Moortgat-Pick *et al.*, arXiv:hep-ph/0507011.

[13] B. Badelek *et al.* [ECFA/DESY Photon Collider Working Group Collaboration], Int. J. Mod. Phys. A **19** (2004) 5097 [arXiv:hep-ex/0108012].

[14] M. M. Muhlleitner and P. M. Zerwas, Acta Phys. Polon. B **37** (2006) 1021 [arXiv:hep-ph/0511339].

[15] A. Djouadi, arXiv:hep-ph/0503172; M. Gomez-Bock, M. Mondragon, M. Muhlleitner, R. Noriega-Papaqui, I. Pedraza, M. Spira and P. M. Zerwas, J. Phys. Conf. Ser. **18** (2005) 74 [arXiv:hep-ph/0509077]; S. Dawson, arXiv:hep-ph/0510385.

[16] S. Heinemeyer *et al.*, 2005 Snowmass Workshop, arXiv:hep-ph/0511332.

[17] M. W. Grunewald, arXiv:0709.3744 [hep-ex].

[18] R. Barate *et al.* [LEP Working Group for Higgs boson searches], Phys. Lett. B **565** (2003) 61 [arXiv:hep-ex/0306033].

[19] F. Gianotti, Talk at the Lepton-Photon Symposium, Uppsala 2005.

[20] M. Duhrssen, S. Heinemeyer, H. Logan, D. Rainwater, G. Weiglein and D. Zeppenfeld, Phys. Rev. D **70** (2004) 113009 [arXiv:hep-ph/0406323].

[21] W. Lohmann, private communication, and P. Garcia-Abia and W. Lohmann, Eur. Phys. J. directC **2** (2000) 2 [arXiv:hep-ex/9908065].

[22] M. Battaglia and K. Desch, arXiv:hep-ph/0101165.

[23] S. Yamashita, Talk at LCWS 2005, Stanford CA.

[24] A. Djouadi, W. Kilian, M. Muhlleitner and P. M. Zerwas, Eur. Phys. J. C **10** (1999) 27 [arXiv:hep-ph/9903229].

[25] U. Baur, T. Plehn and D. L. Rainwater, Phys. Rev. D **67** (2003) 033003 [arXiv:hep-ph/0211224].

[26] V. Barger, T. Han, P. Langacker, B. McElrath and P. Zerwas, Phys. Rev. D **67** (2003) 115001 [arXiv:hep-ph/0301097].

[27] M. M. Muhlleitner, M. Kramer, M. Spira and P. M. Zerwas, Phys. Lett. B **508** (2001) 311 [arXiv:hep-ph/0101083].

[28] K. Desch, T. Klimkovich, T. Kuhl and A. Raspereza, arXiv:hep-ph/0406229.

[29] P. Niezurawski, A. F. Zarnecki and M. Krawczyk, arXiv:hep-ph/0507006.

[30] S. Heinemeyer, W. Hollik and G. Weiglein, arXiv:hep-ph/0412214.

[31] A. Juste *et al.*, 2005 Snowmass Workshop, arXiv:hep-ph/0601112.

[32] D. J. Miller, R. Nevzorov and P. M. Zerwas, Nucl. Phys. B **681** (2004) 3 [arXiv:hep-ph/0304049].

[33] J. F. Gunion and M. Szleper, arXiv:hep-ph/0409208.

[34] U. Ellwanger, J. F. Gunion, C. Hugonie and S. Moretti, arXiv:hep-ph/0401228.

[35] E. Farhi and L. Susskind, Phys. Rev. D **20** (1979) 3404; E. Eichten and K. D. Lane, Phys. Lett. B **90** (1980) 125; see also the reviews: C. T. Hill and E. H. Simmons, Phys. Rept. **381** (2003) 235 [Erratum-ibid. **390** (2004) 553] [arXiv:hep-ph/0203079]; W. Kilian, Springer tracts in modern physics **198** (2003).

[36] N. Arkani-Hamed, A. G. Cohen, H. Georgi, Phys. Lett. B **513** (2001) 232 [arXiv:hep-ph/0105239]; N. Arkani-Hamed, A. G. Cohen, T. Gregoire, and J. G. Wacker, JHEP **0208** (2002) 020. [arXiv:hep-ph/0202089]; N. Arkani-Hamed, A. G. Cohen, E. Katz, and A. E. Nelson, JHEP **0207** (2002) 034. [arXiv:hep-ph/0206021]; M. Schmaltz, JHEP **0408** (2004) 056; for reviews, see: M. Schmaltz and D. Tucker-Smith, arXiv:hep-ph/0502182; M. Perelstein, arXiv:hep-ph/0512128.

[37] T. Han, H. E. Logan, B. McElrath, and L.-T. Wang, Phys. Rev. D **67** (2003) 095004. [arXiv:hep-ph/0301040]; W. Kilian and J. Reuter, Phys. Rev. D **70** (2004) 015004 [arXiv:hep-ph/0311095]; T. Han, H. E. Logan, B. McElrath and L. T. Wang, Phys. Lett. B **563** (2003) 191 [Erratum-ibid. B **603** (2004) 257] [arXiv:hep-ph/0302188].

[38] J. A. Conley, J. Hewett and M. P. Le, Phys. Rev. D **72** (2005) 115014 [arXiv:hep-ph/0507198].

[39] W. Kilian, D. Rainwater and J. Reuter, Phys. Rev. D **71** (2005) 015008 [arXiv:hep-ph/0411213].

[40] T. Appelquist and C. Bernard, Phys. Rev. D22, 200 (1980); A. Longhitano, Phys. Rev. D22, 1166 (1980); Nucl. Phys. B188, 118 (1981); T. Appelquist and G. H. Wu, Phys. Rev. D **48** (1993) 3235 [arXiv:hep-ph/9304240].

[41] E. Boos, H. J. He, W. Kilian, A. Pukhov, C. P. Yuan and P. M. Zerwas, Phys. Rev. D **57** (1998) 1553 [arXiv:hep-ph/9708310], and Phys. Rev. D **61** (2000) 077901 [arXiv:hep-ph/9908409].

[42] R. Chierici, S. Rosati, and M. Kobel, LC-PHSM-2001-038.

[43] P. Krstonosic, K. Monig, M. Beyer, E. Schmidt and H. Schroder, arXiv:hep-ph/0508179.

[44] J. F. Gunion, arXiv:hep-ph/0410379.

[45] K. m. Cheung, Phys. Rev. D **63** (2001) 056007 [arXiv:hep-ph/0009232].

[46] F. J. Petriello, JHEP **0205** (2002) 003 [arXiv:hep-ph/0204067].

[47] C. Csaki, C. Grojean, H. Murayama, L. Pilo and J. Terning, Phys. Rev. D **69** (2004) 055006 [arXiv:hep-ph/0305237]; C. Csaki, C. Grojean, L. Pilo and J. Terning, Phys. Rev. Lett. **92** (2004) 101802 [arXiv:hep-ph/0308038]

[48] A. Birkedal, K. Matchev and M. Perelstein, Phys. Rev. Lett. **94** (2005) 191803 [arXiv:hep-ph/0412278], and arXiv:hep-ph/0508185.

[49] H. P. Nilles, Phys. Rept. **110** (1984) 1; H. E. Haber and G. L. Kane, Phys. Rept. **117** (1985) 75.

[50] J. R. Ellis, S. Heinemeyer, K. A. Olive, A. M. Weber and G. Weiglein, arXiv:0706.0652 [hep-ph].

[51] J. A. Aguilar-Saavedra *et al.* [SPA Project Collaboration], arXiv:hep-ph/0511344.

[52] G. Weiglein *et al.* [LHC/LC Study Group Collaboration], arXiv:hep-ph/0410364.

[53] B. C. Allanach, G. A. Blair, S. Kraml, H. U. Martyn, G. Polesello, W. Porod and P. M. Zerwas, arXiv:hep-ph/0403133 and arXiv:hep-ph/0512084.

[54] R. Lafaye, T. Plehn and D. Zerwas, arXiv:hep-ph/0404282; R. Lafaye, T. Plehn, M. Rauch and D. Zerwas, arXiv:0709.3985 [hep-ph]; P. Bechtle, K. Desch and P. Wienemann, Comput. Phys. Commun. **174** (2006) 47 [arXiv:hep-ph/0412012].

[55] B. C. Allanach *et al.*, Eur. Phys. J. C **25** (2002) 113 [arXiv:hep-ph/0202233].

[56] B. K. Gjelsten, D. J. Miller and P. Osland, JHEP **0412** (2004) 003 [arXiv:hep-ph/0410303]; JHEP **0506** (2005) 015 [arXiv:hep-ph/0501033]; and arXiv:hep-ph/0510356.

[57] A. Freitas, A. von Manteuffel and P. M. Zerwas, Eur. Phys. J. C **34** (2004) 487 [arXiv:hep-ph/0310182], and Eur. Phys. J. C **40** (2005) 435 [arXiv:hep-ph/0408341]; A. Freitas, D. J. Miller and P. M. Zerwas, Eur. Phys. J. C **21** (2001) 361 [arXiv:hep-ph/0106198]; see also J. L. Feng and M. E. Peskin, Phys. Rev. D **64** (2001) 115002 [arXiv:hep-ph/0105100].

[58] H. U. Martyn, arXiv:hep-ph/0406123.

[59] A. J. Barr, Phys. Lett. B **596** (2004) 205 [arXiv:hep-ph/0405052]; J. M. Smillie and B. R. Webber, JHEP **0510** (2005) 069 [arXiv:hep-ph/0507170]; A. J. Barr, arXiv:hep-ph/0511115.

[60] S. Y. Choi, K. Hagiwara, H. U. Martyn, K. Mawatari and P. M. Zerwas, Eur. Phys. J. C **51** (2007) 753 [arXiv:hep-ph/0612301].

[61] S. Y. Choi, A. Djouadi, M. Guchait, J. Kalinowski, H. S. Song and P. M. Zerwas, Eur. Phys. J. C **14** (2000) 535 [arXiv:hep-ph/0002033].

[62] S. Y. Choi, J. Kalinowski, G. Moortgat-Pick and P. M. Zerwas, Eur. Phys. J. C **22** (2001) 563 [Addendum-ibid. C **23** (2002) 769] [arXiv:hep-ph/0108117].

[63] A. Bartl, H. Eberl, S. Kraml, W. Majerotto and W. Porod, Eur. Phys. J. directC **2** (2000) 6 [arXiv:hep-ph/0002115]; A. Finch, A. Sopczak and H. Nowak, "A scalar top study with c-quark tagging at a linear e+ e- collider," LC-PHSM-2003-075 and Int. Europhysics Conference HEP(2003), Aachen.

[64] A. Freitas, P. Z. Skands, M. Spira and P. M. Zerwas, JHEP **0707** (2007) 025 [arXiv:hep-ph/0703160].

[65] G. A. Blair, W. Porod and P. M. Zerwas, Phys. Rev. D **63** (2001) 017703 [arXiv:hep-ph/0007107], and Eur. Phys. J. C **27** (2003) 263 [arXiv:hep-ph/0210058].

[66] J. R. Ellis, S. Kelley and D. V. Nanopoulos, Phys. Lett. B **260** (1991) 131; P. Langacker and M. x. Luo, Phys. Rev. D **44** (1991) 817; U. Amaldi, W. de Boer and H. Furstenau, Phys. Lett. B **260** (1991) 447.

[67] P. Minkowski, Phys. Lett. B **67** (1977) 421; T. Yanagida, *In Proceedings of the Workshop on the Baryon Number of the Universe and Unified Theories, Tsukuba, Japan, 1979*; M. Gell-Mann, P. Ramond and R. Slansky, *In Proceedings "Supergravity", North Holland, 1979.*

[68] A. Freitas, W. Porod and P. M. Zerwas, Phys. Rev. D **72** (2005) 115002 [arXiv:hep-ph/0509056].

[69] H. Baer, M. Brhlik, M. A. Diaz, J. Ferrandis, P. Mercadante, P. Quintana and X. Tata, Phys. Rev. D **63** (2001) 015007 [arXiv:hep-ph/0005027].

[70] F. Deppisch, A. Freitas, W. Porod and P. M. Zerwas, *in preparation.*

[71] N. Arkani-Hamed and S. Dimopoulos, JHEP **0506** (2005) 073 [arXiv:hep-th/0405159]; G. F. Giudice and A. Romanino, Nucl. Phys. B **699** (2004) 65 [Erratum-ibid. B **706** (2005) 65] [arXiv:hep-ph/0406088]; N. Arkani-Hamed, S. Dimopoulos, G. F. Giudice and A. Romanino, Nucl. Phys. B **709** (2005) 3 [arXiv:hep-ph/0409232].

[72] W. Kilian, T. Plehn, P. Richardson and E. Schmidt, Eur. Phys. J. C **39** (2005) 229 [arXiv:hep-ph/0408088].

[73] A. C. Kraan, J. B. Hansen and P. Nevski, arXiv:hep-ex/0511014.

[74] A. Pierce, Phys. Rev. D **70** (2004) 075006 [arXiv:hep-ph/0406144].

[75] P. Binetruy, M. K. Gaillard and B. D. Nelson, Nucl. Phys. B **604** (2001) 32 [arXiv:hep-ph/0011081].

[76] S. Godfrey, P. Kalyniak and A. Tomkins, 2005 Snowmass Workshop, arXiv:hep-ph/0511335, and *private communication.*

[77] S. Riemann, Note LC-TH-2001-007.

[78] S. Godfrey, P. Kalyniak and A. Tomkins, arXiv:hep-ph/0511335.

[79] M M. Battaglia, A. De Roeck, J. Ellis and D. Schulte (eds.), [CLIC Physics Working Group], CERN-2004-005.

[80] G. F. Giudice, R. Rattazzi and J. D. Wells, Nucl. Phys. B **544** (1999) 3 [arXiv:hep-ph/9811291].

[81] G. Wilson in Ref. [2].

[82] H. Davoudiasl, J. L. Hewett and T. G. Rizzo, Phys. Rev. Lett. **84** (2000) 2080 [arXiv:hep-ph/9909255].

[83] J. L. Feng, arXiv:hep-ph/0509309.

[84] M. Fukugita and T. Yanagida, Phys. Lett. B **174** (1986) 45.

[85] W. Buchmuller, P. Di Bari and M. Plumacher, Nucl. Phys. B **665** (2003) 445 [arXiv:hep-ph/0302092].

[86] M. Carena, M. Quiros and C. E. M. Wagner, Phys. Lett. B **380** (1996) 81 [arXiv:hep-ph/9603420].

[87] M. Carena, A. Finch, A. Freitas, C. Milstene, H. Nowak and A. Sopczak, Phys. Rev. D **72** (2005) 115008 [arXiv:hep-ph/0508152].

[88] D. N. Spergel *et al.* [WMAP Collaboration], Astrophys. J. Suppl. **148** (2003) 175 [arXiv:astro-ph/0302209].

[89] M. Battaglia, Talk at LCWS 2005, Stanford CA.

[90] P. Bambade, M. Berggren, F. Richard and Z. Zhang, arXiv:hep-ph/0406010; H. U. Martyn, arXiv:hep-ph/0408226; V. Khotilovich, R. Arnowitt, B. Dutta and T. Kamon, Phys. Lett. B **618** (2005) 182 [arXiv:hep-ph/0503165].

[91] G. Polesello and D. R. Tovey, JHEP **0405** (2004) 071 [arXiv:hep-ph/0403047]; M. M. Nojiri, G. Polesello and D. R. Tovey, arXiv:hep-ph/0512204.

[92] E. A. Baltz, M. Battaglia, M. E. Peskin and T. Wizansky, Phys. Rev. D **74** (2006) 103521 [arXiv:hep-ph/0602187].

[93] H. Pagels and J. R. Primack, Phys. Rev. Lett. **48** (1982) 223; M. Y. Khlopov and A. D. Linde, Phys. Lett. B **138** (1984) 265; J. R. Ellis, J. E. Kim and D. V. Nanopoulos, Phys. Lett. B **145** (1984) 181; M. Bolz, W. Buchmuller and M. Plumacher, Phys. Lett. B **443** (1998) 209 [arXiv:hep-ph/9809381].

[94] F. D. Steffen, AIP Conf. Proc. **903** (2007) 595 [arXiv:hep-ph/0611027].

[95] W. Buchmuller, K. Hamaguchi, M. Ratz and T. Yanagida, Phys. Lett. B **588** (2004) 90 [arXiv:hep-ph/0402179]; J. L. Feng, S. Su and F. Takayama, Phys. Rev. D **70** (2004) 075019 [arXiv:hep-ph/0404231]; A. De Roeck, J. R. Ellis, F. Gianotti, F. Moortgat, K. A. Olive and L. Pape, arXiv:hep-ph/0508198; H. U. Martyn, Eur. Phys. J. C **48** (2006) 15 [arXiv:hep-ph/0605257].